NASA Technical Paper 2232

April 1984

Review and Status of Heat-Transfer Technology for Internal Passages of Air-Cooled Turbine Blades

Frederick C. Yeh
and Francis S. Stepka

NASA

NASA
Technical
Paper
2232

1984

Review and Status of Heat-Transfer Technology for Internal Passages of Air-Cooled Turbine Blades

Frederick C. Yeh
and Francis S. Stepka

Lewis Research Center
Cleveland, Ohio

NASA
National Aeronautics
and Space Administration

**Scientific and Technical
Information Branch**

Summary

A review of turbine-blade coolant-side heat-transfer technology is needed as inaccuracies in many of the correlations or extrapolations of correlations can result in large errors in the prediction of turbine-blade metal temperatures and life. Designers have often used correlating heat-transfer and flow equations because of a general acceptance of its usage and do not have the time to inquire about the inaccuracies of the correlations, the conditions, and the range of applicability.

This review indicated that even for ideal conditions the correlations for heat transfer and pressure drop were at best about ±10 percent accurate and some approached ±35 percent error. Further research is needed to provide needed data and improved accuracy of predictions for local turbulent heat transfer and pressure drops for inlet regions of passages, noncircular passages with and without turbulators (ribs and pins), impingement cooling coupled with film injection of the coolant, and, particularly, for passages under conditions of rotation.

Introduction

Much information has been obtained on the heat-transfer coefficients and pressure losses of airflow through passages. More continues to be obtained to extend the range of conditions, determine the effect of variations of cooling methods and configurations, and improve the accuracy of the equations that correlate the data. Those working directly with cooling of turbines have organized and condensed much of the information and have selected correlations they consider most appropriate to their usage and cooling methods. However, much of this information is proprietary. Those who do not have access to the proprietary data must rely on published literature. Designers generally use correlating equations because of the general acceptance of their usage, and often extrapolate these equations beyond their range of applicability. A review of coolant-side heat-transfer technology is needed as inaccuracies in some of the correlations used or extrapolations of these correlations can result in large errors in the prediction of turbine-blade metal temperatures and life. Even a ±10 percent inaccuracy in the coolant-side heat-transfer coefficient can mean an uncertainty of ±15 K (27° F) in the surface metal temperature of an advanced turbine-blade design (ref. 1). This uncertainty in metal temperature can affect blade life by a factor of about 2.

The purposes of this study were to (1) review some published literature on heat transfer and pressure losses of air flow through passages for several cooling methods generally applicable to gas turbine blades, (2) select the more useful correlating equations for coolant passages in nonrotating and rotating blades, (3) assess the status of turbine-blade internal air-cooling technology, and (4) describe areas where further research is needed. The cooling methods considered include convection cooling, impingement cooling at the leading edge and at the midchord, and convection cooling augmented by pins and internal ribs. Also in this study, emphasis was placed on turbulent flows because turbulent flow is generally needed to promote the high degree of blade cooling required in gas-turbine engines. Transpiration cooling and film cooling, although important to the cooling of advanced turbines, were not considered in this study.

Symbols

A	area
$\bar{A}$	flow area in pin array section, $=v/L$
A_0^*	ratio of jet hole area to opposing impingement surface area (open area ratio)
$\mathfrak{A}$	correlation function for impingement heat transfer on flat plate (eq. (37))
a	correlation constants (eqs. (34) to (36); also see table IV)
B	dimensionless quantity, $B=\left(\sqrt{2}A_0^*C_dL\right)/z$
$\mathfrak{B}$	correlation function for impingement heat transfer on flat plate (eq. (37))
b	width of an equivalent two-dimensional nozzle having equal flow area, $=\pi d^2/4c$; correlation constant (eqs. (34) and (35); also see table IV)
C	correlation constant
C_d	coefficient of discharge
c	center-to-center distance between impingement holes; correlation constant (eqs. (34) and (35)); also see table IV)
c_p	specific heat
D	pipe inside diameter
D_h	hydraulic diameter $=4A/\mathcal{P}$; for impingement cooling in leading edge cavity, $=2bc(n-1)/[b+c(n-1)]$
D'	characteristic diameter as defined after eqs. (51) and (54)
D_{eff}	effective pipe diameter $=4l/\pi$
d	impingement hole diameter; pin fin diameter
e	height of turbulators
e^+	roughness Reynolds number, $\equiv eu^*/\nu$ $=(e/D)\text{Re}\sqrt{f/2}$
f	friction factor
G	mass flow rate per unit area, $=W/A$
g	heat-transfer function, $=[f/(2\text{St})-1]/\sqrt{f/2}+u_e^+$

$\bar{g}$	$\equiv g\ \mathrm{Pr}^{-0.57}$
H	enthalpy
h	heat-transfer coefficient
i,j	correlation exponents (eq. (47))
K	geometry factor for turbulent flow; total pressure loss coefficient
k	thermal conductivity
L	length of flow passage; length of pin array section or jet-impingement plate in streamwise direction
l	half arc length of leading-edge cavity from stagnation point; pin fin height
M	Mach number; initial crossflow to total jet flow ratio, $= W_c/W_j$
m	correlation function or constant for eqs. (33), (37), and (48)
Nu	Nusselt number, $= hD/k$ for pipe flow, $= hd/k$ for impingement flow
n	correlation exponent (eqs. (37), (39), and (48)); number of impingement holes in a single spanwise row in leading edge cavity
P	pressure
Pr	Prandtl number
$\mathcal{P}$	wetted perimeter
p_t	center-to-center distance between turbulators
p_p	center-to-center distance between pins on triangular pitch
$q+$	heat flux parameter $= q''(GH_{o,i})$
q''	heat flux
R	recovery factor
Ra	rotational Rayleigh number, $= \Omega^2\beta r^4\tau/\nu\alpha$
Re	Reynolds number, $= DG/\mu$
Re_w	modified wall Reynolds number, $= (DG/\mu)(\rho_w/\rho_b)$
Re_Ω	rotational Reynolds number, $= \Omega D^2/\nu$
r	tube radius
S	Rossby number, $= \Omega D/V_m$
$\mathcal{S}$	total heat-transfer surface area (exposed wall area + pin area)
St	Stanton number
T	temperature
t	wall thickness
u_e^+	roughness function, $= \sqrt{2/f} + 2.5\ \ln(2e/D) + 3.75$
u^*	friction velocity, $\equiv \sqrt{\tau_0/\rho}$
V	velocity
v	open volume in pin array section
W	mass flow rate
x	distance along pipe from inlet or impingement plate leading edge
$\tilde{x}$	x/L
$\tilde{x}'$	$= \tilde{x} - (1/2)(x_n/L)$
x_n, y_n	streamwise or spanwise jet hole spacing
x_p, y_p	streamwise or spanwise pin fin spacing
z	distance between impingement jet hole and target surface
α	thermal diffusivity, $= k/\rho c$; included angle in triangular duct
β	expansion coefficient
δ	flow angle of attack
ζ	function defined in eq. (41)
θ	rib shape angle
μ	dynamic viscosity
ν	kinematic viscosity
ρ	density
τ	wall axial temperature gradient
τ_o	apparent wall shear stress
φ	correlation function for impingement heat transfer (eq. (33))
Ω	angular velocity
{ }	as a function of

Subscripts:

a	based on velocity arriving at the target plate
aw	adiabatic wall
b	at bulk temperature
c	cross flow
cp	constant properties
d	based on impingement hole diameter
eq	evaluated using equivalent slot width
f	at film temperature
m	mean
max	maximum
min	minimum
mod	modified
n	nozzle
i	initial condition
j	jet
l	at arc length from leading edge stagnation line
o	stagnation condition
p	pin fin
r	reference
s	stationary; static
t	turbulent
tot	total
w	wall

x distance from duct inlet; streamwise direction

y spanwise direction

z direction normal to impingement target surface

Superscripts:

nx exponent associated with geometry in streamwise direction

ny exponent associated with geometry in spanwise direction

nz exponent associated with geometry normal to impingement surface

Passages of Air-Cooled Blades

For those in the heat-transfer community not directly involved with the cooling of gas turbines, a brief description of the general types of cooled passages and methods may be helpful. Typical turbine airfoils incorporate passages that provide cooling by a number of methods. Figure 1(a) shows an example of an airfoil design that uses radial passages for simple convective cooling. The passages may be circular, rectangular, or triangular in cross section.

A more complex internal geometry may incorporate several cooling schemes. The midchord region of the airfoil shown in figure 1(b) is convectively cooled by radial flow of cooling air through generally rectangular passages. The cooling air generally makes a number of return flows in the adjacent passages before exiting the airfoil. The radial flow channels are shown in the figure as having smooth walls. Generally, however, raised ribs normal, or at some angle to the direction of airflow are provided on the pressure and suction surfaces of the airfoil. These ribs, often refered to as turbulaters, break up the boundary layer and increase heat transfer. This type of airfoil design is often referred to as the multipass cooled configuration. At the trailing-edge cooling airflows through chordwise channels before exiting the airfoil. Often arrays of short cylindrical or eliptical pins are added in this region to increase structural strength as well as to act as turbulators to increase heat transfer.

The leading-edge area of the turbine airfoil is generally more difficult to cool than other areas because of the very high heat-transfer rates encountered in the gas stream at the stagnation area. Impingement cooling (e.g., fig. 1(b)) is often used. In this cooling method cooling air from the forward flow channel flows through single or multiple rows of holes to impinge on the inner surface of the leading-edge wall. The cooling air is then routed within the airfoil or ejected from holes in the leading-edge walls to further protect the blade with a film of cooling air.

Often the impingement cooling method is used at the midchord region of turbine vanes (fig. 1(c)). In this method cooling air exits from a large array of holes in a sheet metal insert in the center of the airfoil to impinge on most of the airfoil inner surfaces before exiting the airfoil through chordwise channels, arrays of pins, or film cooling holes at the trailing-edge region.

Both nonrotating turbine vanes and rotating blades use this cooling scheme in its various forms or in combinations with other schemes. Although frequently not accounted for in the thermal designs, the effects of rotation must be understood to improve blade passage design. At the high rotational speeds encountered in aircraft turbines, the Coriolis forces generate secondary forces within the flow channels. In addition, free-convection heat transfer could become significant because of the buoyancy forces caused by the density gradients and high centrifugal forces generated. Typical rotational speeds and acceleration levels for advanced large gas turbines are of the order of 17 000 rpm and 75 000 g's, and for small turbines of the order of 65 000 rpm and 400 000 g's. Figure 1(d) illustrates a simple radial passage design in a rotating turbine blade. Since the pressure and suction-side walls of the turbine at the

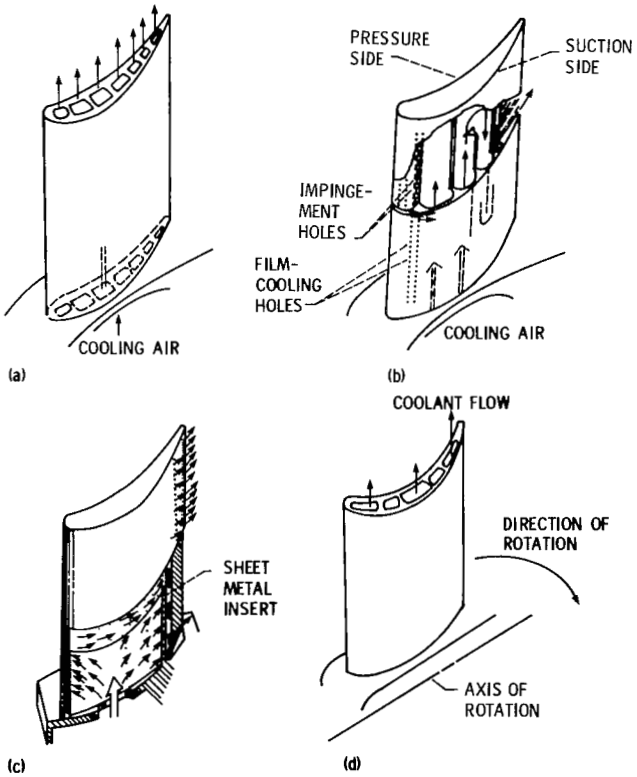

(a) Simple convective cooling.
(b) Cooled by several methods.
(c) Impingement cooled vane.
(d) Rotating blade.

Figure 1. – Cooled turbine airfoils.

midchord are shown parallel to the axis of rotation, the Coriolis forces would act on the fluid in a direction normal to these two walls. However, at the trailing or leading edge, where the suction and pressure surfaces are not parallel to the axis of rotation, the Coriolis forces will act on the fluid in a direction that is not normal to these walls. The secondary flow patterns within the passages would be expected to differ depending on the location of the flow channels.

Convection Cooling

Simple convective cooling is currently used only in older turbines, or in applications where the turbine-inlet temperatures and heat load demands are low and where more complex cooling geometries are either physically impractical or economically unjustifiable. In some advanced applications simple convective cooling can still be used in conjunction with external ceramic coatings, which shield and insulate the blade metal from the hot gas (ref. 2). Simple convective cooling may also be used in applications where the air is precooled below compressor-exit bleed temperatures by a heat exchanger or by the injection of water (and use of its latent heat of vaporization).

In simple convective cooling, cooling air generally flows in the radial direction (fig. 1(a)). In certain instances, however, the cooling air is made to flow in the axial direction.

Most experimental investigations of forced-convection cooling have been performed in long, circular tubes and under conditions of fully developed velocity profiles entering the heat-transfer test section. Such carefully established inlet conditions help contribute reproducibility in the experimental results. However, the coolant passages in turbine blades pose flow and geometry conditions quite different from those maintained in most forced-convection heat-transfer investigations: Velocity profiles are not fully developed and the passage cross-sectional shape is apt to be noncircular. In evaluating the analysis methods or correlations available for turbine cooling application, it is necessary to examine the extensive literature on fully developed convective heat transfer. Consequently, this literature will be cited and discussed herein. Utilizing entrance effect studies and other studies pertaining to coolant passage geometry in combination with fully developed predictions, it may be possible to obtain thermal design procedures relevant to turbine blade or vane geometries. In addition, recommendations are made herein for further heat-transfer research to reduce the uncertainty in thermal design predictions.

Circular Passages

Simple convective heat transfer through circular pipes has been extensively investigated, giving both empirical correlations and analytical formulations (e.g., refs. 3 to 29).

Siegel and Sparrow (ref. 3) addressed the question of how heat transfer varies in turbulent flow under boundary conditions of uniform wall temperature and uniform wall heat flux. They found that, for a circular pipe, the turbulent heat-transfer mechanism in the fully developed and in the thermal entrance regions are insensitive to these two boundary conditions for Prandtl numbers equal to or greater than 0.7. Therefore, the boundary conditions most often used do not significantly alter the test results or correlations when air is used as the fluid.

One of the earliest correlations for fully developed turbulent flow in smooth circular pipes and for constant physical properties is due to Dittus and Boelter (ref. 4):

$$\mathrm{Nu} = 0.023\ \mathrm{Re}^{0.8}\mathrm{Pr}^{0.4} \tag{1}$$

where fluid properties were evaluated at the bulk temperatures.

In recent years, a correlation for constant physical properties due to Petukhov and Popov (ref. 5) has also been used:

$$\mathrm{Nu} = \frac{(f/8)\mathrm{Re}\ \mathrm{Pr}}{1.07 + 12.7\sqrt{f/8}(\mathrm{Pr}^{2/3} - 1)} \tag{2}$$

where f is the friction factor, which may be calculated from the Prandtl-Karman equation:

$$\frac{1}{\sqrt{f}} = 2\log\left(\mathrm{Re}\sqrt{f}\right) - 0.8 \tag{3}$$

Because of its simplicity and long standing usage, the Dittus-Boelter correlation has remained a favorite with which other correlations are compared. The correlation still gives satisfactory results for circular passages and other passage geometries that are not too extreme (e.g., very small included angles), and for nearly constant fluid physical properties. (Such would be the case if the heat flux were moderate and if the ratio of gas to coolant temperature were only slightly different from 1.) In turbine cooling applications the geometry of the coolant passages are frequently noncircular, the turbine-inlet temperatures are of the order of 1650 K (2500° F) or higher, the heat fluxes of the order of 5.5×10^6 watts per square meter, and wall-to-coolant temperature ratios of the order of 2.5 to 1. Under these conditions, the assumption of constant physical properties is no longer valid, and the predicted heat-transfer coefficients can be in considerable error (of the order of $\sqrt{T_b/T_w}$.

Considerable work, both analytical and experimental, has been done in the area of variable physical properties or varying heating conditions (refs. 7 to 27). The experimental data covered both passage-length-averaged and circumferentially averaged axial heat-transfer coefficients. Many of the cited references report research conducted for nuclear reactor applications where hydrogen or helium is frequently used and where the surface-to-bulk temperature ratios considerably exceed those found in turbine-blade designs. The assumption made in these correlations is that the gas is chemically frozen; that is, chemical reaction is not included. In general, the equation correlating the experimental data take the form

$$\mathrm{Nu} = C\,\mathrm{Re}^{0.8}\mathrm{Pr}^{b}\left(\frac{T_w}{T_b}\right)^{-n} \tag{4}$$

with an L/D or x/D dependence and where the Nusselt number is the circumferentially averaged local value at the axial distance x from the entrance. Either bulk or film properties can be used to obtain a correlation. The effect of the variable properties is accounted for by $(T_w/T_b)^{-n}$ where $n \approx 1/2$. and $b \approx 0.4$. When $n = 0$, equation (4) reverts to the familiar form of the Dittus-Boelter equation. Equation (4) indicates that the heat-transfer coefficient decreases as the wall-to-bulk temperature ratio increases.

McEligot, Magee, and Leppert (ref. 8) reported on the effect of wall-to-bulk temperature ratios on heat transfer and pressure drop. The experiments covered a range of wall-to-bulk temperature ratios from unity to 2.5, and Reynolds numbers based on bulk properties at pipe inlet conditions from 1.5×10^4 to 2.33×10^5. The experimental data on average heat-transfer coefficient with properties based on bulk temperatures agreed favorably with Taylor (ref. 9) and other investigators and correlated with the following equation:

$$\mathrm{Nu}_b = 0.021\,\mathrm{Re}_b^{0.8}\mathrm{Pr}_b^{0.4}\left(\frac{\bar{T}_w}{\bar{T}_b}\right)^{-0.5} \tag{5}$$

Local heat-transfer coefficients were correlated to about 13 percent by the following correlation, except for the first few diameters of length:

$$\mathrm{Nu} = 0.021\,\mathrm{Re}^{0.8}\mathrm{Pr}^{0.4}\left(\frac{T_w}{T_b}\right)^{-0.5}\left[1 + \left(\frac{x}{D}\right)^{-0.7}\right] \tag{6}$$

for $x/D > 5$, where Nu is the local Nusselt number at an axial distance x from the entrance. The equation is valid for $1.5 \times 10^4 < \mathrm{Re} < 6.0 \times 10^5$ (based on bulk properties), $0 < q^+ < 0.004$, $1 < (T_w/T_b) < 2.4$, and 350 K (170° F) $< T_w <$ 360 K (190° F). The heat flux parameter q^+ defined as

$$q^+ = \frac{q''}{(GH_{o,i})} \tag{7}$$

Comparison of the above correlation with their experimental data showed agreement to about 13 percent.

Taylor conducted experiments using precooled helium and hydrogen, with surface to bulk temperature ratios of up to 8, and surface temperatures up to 2950 K (5300° R) (ref. 10). He concluded that the circumferentially averaged heat-transfer coefficients, as a function of the axial distance x from the inlet, can be correlated by the Dalle-Donne equation of reference 17:

$$\mathrm{Nu}_b = 0.021\,\mathrm{Re}_b^{0.8}\mathrm{Pr}_b^{0.4}\left(\frac{T_w}{T_b}\right)^{-[0.29 + 0.0019(x/D)]} \tag{8}$$

where the fluid properties for the calculation of Reynolds, Prandtl, and Nusselt numbers are all evaluated at the bulk temperature. Taylor reported that 90 percent of the hydrogen data correlated to within 10 percent, while 80 percent of the helium data correlated to within 10 percent of the correlation line (fig. 2). Equation (8) is intended for heating in fully developed turbulent flow $(T_w/T_b > 1.0)$. The effect on heat transfer in the

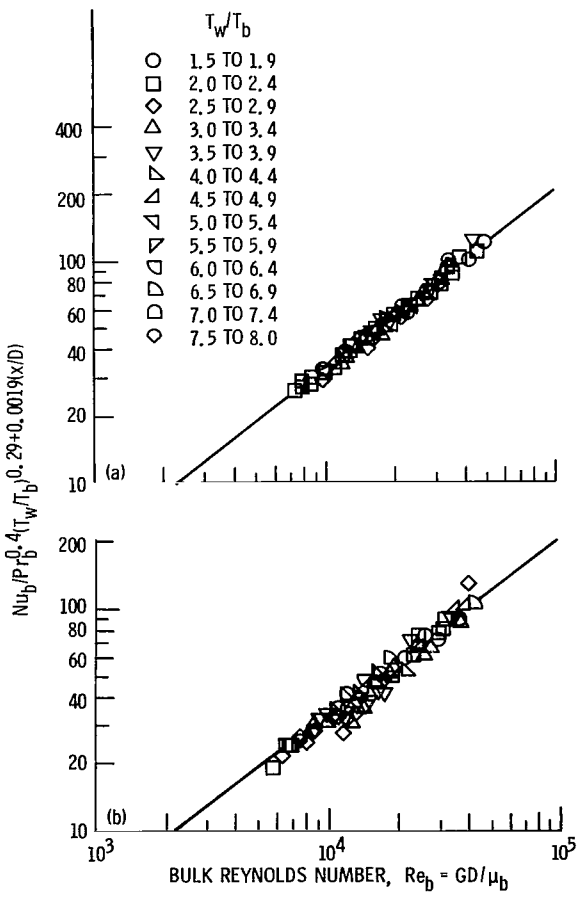

Figure 2. – Correlation of local heat-transfer coefficients using equation (8).

developing region at the entrance of the passages is not included in this correlation.

Petukhov (ref. 19), in an excellent review of heat transfer and friction in turbulent pipe flow, gave the following equation, which was obtained by simplifying an analytical solution for variable properties:

$$\frac{\mathrm{Nu}_b}{\mathrm{Nu}_{cp,b}} = \left(\frac{T_w}{T_b}\right)^n \tag{9}$$

where

$$n = -\left[a \log\left(\frac{T_w}{T_b}\right)\right] + 0.36$$

where $a = 0$ for cooling and 0.3 for heating.

Sleicher and Rouse (ref. 20) examined a number of correlations for constant and variable property heat transfer in turbulent pipe flow. For variable property correlation, they used a constant property correlation developed earlier in the same study. Using a computer code, they determined the modifications necessary to best fit the experimental heat-transfer data of four other investigators (e.g., refs. 15 and 26). Sleicher and Rouse claimed that the following equation for gases gives an average deviation of only 4.2 percent for the data examined, with only 4 of 120 points exceeding 10 percent deviation:

$$\mathrm{Nu}_b = 5 + 0.012\ \mathrm{Re}_b^{0.83}(\mathrm{Pr}_b + 0.29)\left(\frac{T_w}{T_b}\right)^n \tag{10}$$

where $n = -\log(T_w/T_b)^{1/4} + 0.3$. The authors also compared the experimental data with equation (9). Visual examination of the figure given in reference 20 indicated that the average deviation of equation (9) from experimental data appeared to be approximately 10 percent.

Simoneau and Hendricks (ref. 21) correlated several investigators' experimental data for large wall-to-fluid bulk temperature ratios and for four different gases (hydrogen, helium, air, and carbon dioxide). They proposed that the experimental data for the four gases could be correlated by a simple equation if a specific correlation constant C is assigned to a specific gas:

$$h = C(\rho V)_b^{0.8} D^{-0.2}\left(\frac{T_b}{T_w}\right)^{1/2} \tag{11}$$

For air, the constant C has a value of 0.00420. Using this correlation and experimental data from references 7 and 12 for air only, the authors obtained agreement to +11 and −10 percent of the correlating line.

Note that equation (11) contains no fluid transport property terms. Simoneau and Hendricks do not suggest that the physical heat-transfer process is independent of the fluid properties. They merely point out that equation (11) did correlate the experimental data over the wide range of gas temperatures and wall-to-fluid bulk temperature ratios considered.

Black and Sparrow (ref. 22) studied heat-transfer characteristics of turbulent air flow in a circular tube with circumferentially varying wall temperature and heat flux. The imposed circumferential heat flux varied by as much as a factor of 2. Their analysis was based on the method of Sparrow and Lin (ref. 23) and assumed that the thermal diffusivities in the tangential and radial directions were equal. The predicted circumferential variations of Nusselt number and air temperature were shown to be higher than the experimental data. At a Reynolds number of 4.05×10^4 and a circumferential flux variation of ±30 percent about a mean, one of the analyses discussed in reference 23 predicted a circumferential Nusselt number variation of about 36 percent, while the experimental data showed a variation of only about 8 percent. Sparrow and Lin speculated that a higher value of tangential thermal diffusivity than the radial diffusivity may be a more accurate description of the heat-transfer process. When a ratio of tangential to radial thermal diffusivity of 10 is used, the predicted circumferential variations became overly damped and became less than the experimental variations. The authors concluded that these observations lend support to the use of a model wherein the tangential to radial thermal diffusivity is substantially greater than 1 near the wall, but essentially unity elsewhere in the flow.

A comparison of the circumferentially averaged experimental data of reference 22 with the Dittus-Boelter correlation (fig. 3) showed that the data were about 8 percent lower. The comparison showed that even with a circumferential heat flux variation of 2, the Dittus-Boelter correlation provides a good prediction of the average heat-transfer coefficient.

For pressure drop, McEligot, et al., (ref. 8) correlated the friction factor to within about 8 percent of the Karman-Nikuradse equation[1] for x/D greater than 30. For engineering calculations for $x/D > 30$, the authors suggested the following approximate correlation:

$$\frac{f}{f_{cp}} = \left(\frac{T_w}{T_b}\right)^{-0.1} \tag{12}$$

where f_{cp} is the friction factor for adiabatic, constant property conditions determined from the Reynolds number based on local bulk properties.

Taylor (ref. 11) correlated friction coefficients for both laminar and turbulent flow of gases. (See fig. 4.) For

[1]The Karman-Nikuradse equation differs from the Prandtl-Karman equation only in that the former uses the fanning friction factor and the latter uses the Darcy-Weisback friction factor.

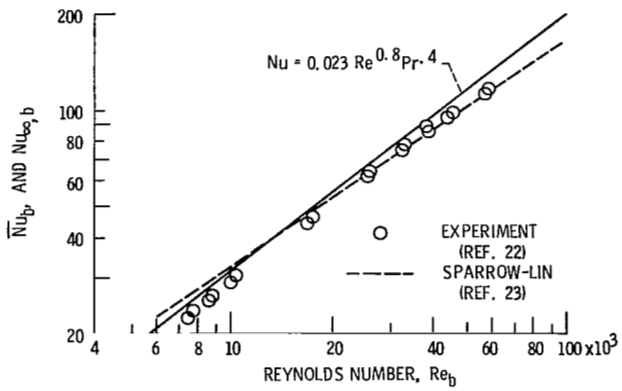

Figure 3. – Comparison of Dittus-Boelter correlation with experimental data on tubes with circumferential heat flux variations as large as 2.0. (From ref. 22.)

turbulent flow he used 423 data points from seven publications (refs. 9, 10, 12 to 15, and 18). The data were for both heating and cooling, for five different gases, including air, for Reynolds numbers from 5.4×10^3 to 1.87×10^5, and for surface-to-fluid bulk temperature ratios from 0.35 to 7.35. Equation (13) correlated 90 percent of the data points to within 10 percent of the correlation (fig. 4(a)). For laminar flow Taylor also reported that equation (14) correlated friction factor for four gases, including air, for Reynolds numbers up to 2.2×10^4, and for surface-to-fluid bulk temperature ratios between 1.0 and 4.1 (fig. 4(b)). For turbulent flow

$$\frac{f}{8} = \left(0.0007 + \frac{0.0625}{\mathrm{Re}_{w,\mathrm{mod}}^{0.32}}\right)\left(\frac{T_b}{T_w}\right)^{0.5} \tag{13}$$

where $\mathrm{Re}_{w,\mathrm{mod}} = GD/\mu_w(T_b/T_w)$. For Laminar flow

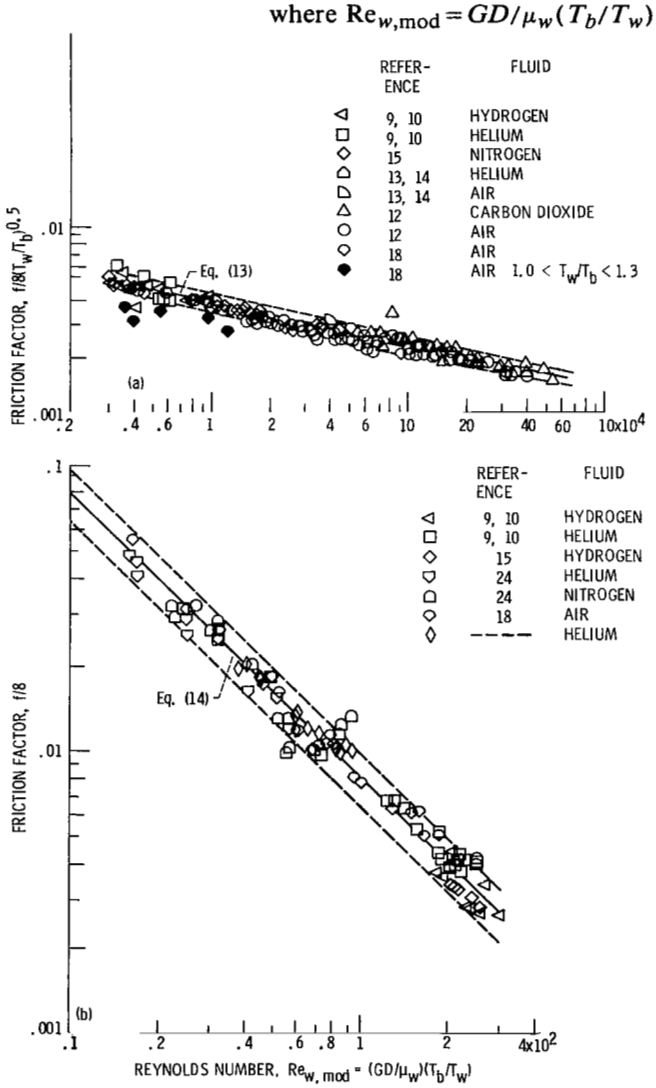

(a) Turbulent flow; 423 points in turbulent region.
(b) Laminar flow; 109 points in laminar region.

Figure 4. – Correlation of average friction factor with density evaluated at bulk temperature and viscosity evaluated at surface temperature. (From ref. 11.)

$$\frac{f}{8} = \frac{8}{\mathrm{Re}_{w,\mathrm{mod}}} \tag{14}$$

Petukhov (ref. 19) gave the following analytic solution for air and hydrogen:

$$\frac{f_b}{f_{b,cp}} = \left(\frac{T_w}{T_b}\right)^n \tag{15}$$

where

$$n = -0.6 + 5.6(\mathrm{Re}_w^*)^{-0.38}$$

and

$$\mathrm{Re}_w^* = \frac{DG}{\mu_w}\left(\frac{\rho_w}{\rho_b}\right)$$

The pressure drop due to friction is defined as

$$\Delta P = \frac{fL}{D}\frac{(\rho V^2)_b}{2g} \tag{16}$$

Noncircular Passages

Noncircular passages are frequently encountered in turbine-blade cooling as well as in many other applications. The prevailing practice is to use the hydraulic diameter ($4A/\mathcal{P}$) and apply it to circular pipe correlations. This procedure is widely used because of its simplicity. If the passage, or duct, geometry is not too extreme, this procedure yields acceptable results in pressure drop and average heat-transfer coefficient for fully developed turbulent flow. If the geometrical configurations become extreme, such as those of triangular cross section, with very small apex angles, then both the pressure drop and average heat-transfer coefficient could deviate unacceptably from the circular duct correlations.

The literature is fairly extensive on flow through noncircular ducts (e.g., refs. 30 to 53). In general, the investigators indicated that the heat transfer in noncircular ducts would be less than that in circular ducts under the same conditions. Pressure drop in noncircular ducts appears to be equal to or less than that in circular ducts at near constant property conditions, but greater than that in circular ducts at variable property conditions.

Deissler and Taylor (ref. 30) presented an analysis of heat transfer and pressure drop for a square duct and an equilateral triangular duct. The analysis, which neglects secondary flows, predicts that for variable fluid properties both the pressure drop and the average heat-transfer coefficient would fall below the values predicted for the circular duct.

Emery, Neighbors, and Gessner (ref. 31) presented a numerical method for calculating turbulent heat transfer in a square duct and concluded that the heat-transfer results were about 10 percent lower than the Dittus-Boelter correlation using hydraulic diameter (fig. 5).

Eckert and Irvine (ref. 32) investigated pressure drop and heat transfer in an isosceles triangle cross section duct with an 11.46° apex angle. For turbulent flow their investigations showed that the friction factor was approximately 20 percent below the circular duct predictions and agreed well with the theoretical predictions of Deissler and Taylor (ref. 30 and fig. 6). For heat transfer the average Nusselt number for the fully developed turbulent flow at 114 hydraulic diameters from the inlet was correlated by the following equation:

$$\mathrm{Nu} = 0.0325\ \mathrm{Re}^{0.66} \tag{17}$$

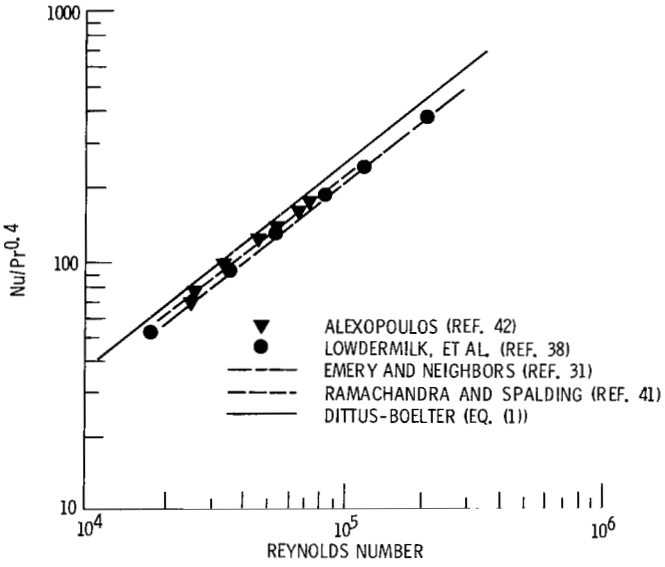

Figure 5. – Comparison of heat transfer in a square duct with Dittus-Boelter equation for circular duct. (From ref. 31.)

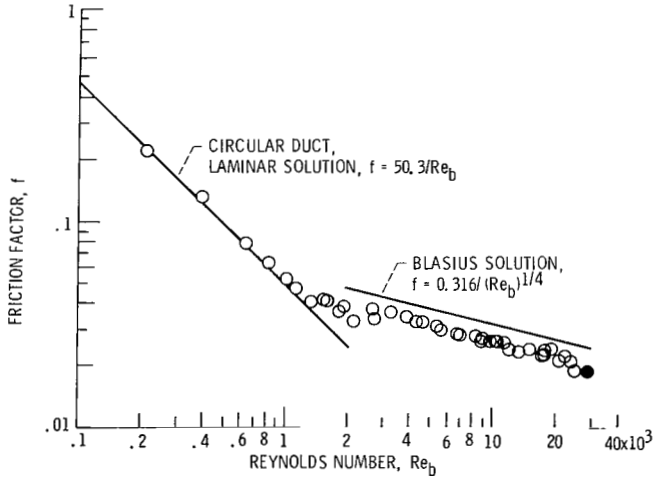

Figure 6. – Fully developed friction factors in 11.46° duct. (From ref. 32.) Solid points calculated by method of Deissler and Taylor (ref. 30).

Properties are evaluated at bulk temperatures and where thermal conditions are fully established.

Figure 7 compares the experimental heat-transfer data of reference 32 and equation (17) with the Dittus-Boelter correlation based on hydraulic diameter. The experimental data were only about one-half as large as the Dittus-Boelter correlation predicts. Eckert and Irving speculated that this difference may result from the turbulent heat diffusivity, on which the heat transport process primarily depends, being much smaller for extremely acute apex angles than for a round duct.

Carlson and Irvine (ref. 33) made a systematic investigation of the friction factors of air in fully developed turbulent flow, using various isosceles triangles with apex angles ranging from 4 to 30. Their results show that the friction factors are generally lower than those predicted for the circular duct and that they vary as a function of the included apex angle (as shown in fig. 8). The authors, therefore, suggested a correlation in the form of a modified Blasius equation

$$f = \frac{C}{\mathrm{Re}^{0.25}} \tag{18}$$

where C is a function of the apex angle (see fig. 9).

Ainsworth and Jones (ref. 34) measured heat-transfer coefficients in circular, rectangular, and triangular ducts, using a short duration transient technique. The triangular duct had an isosceles cross section with an apex angle of

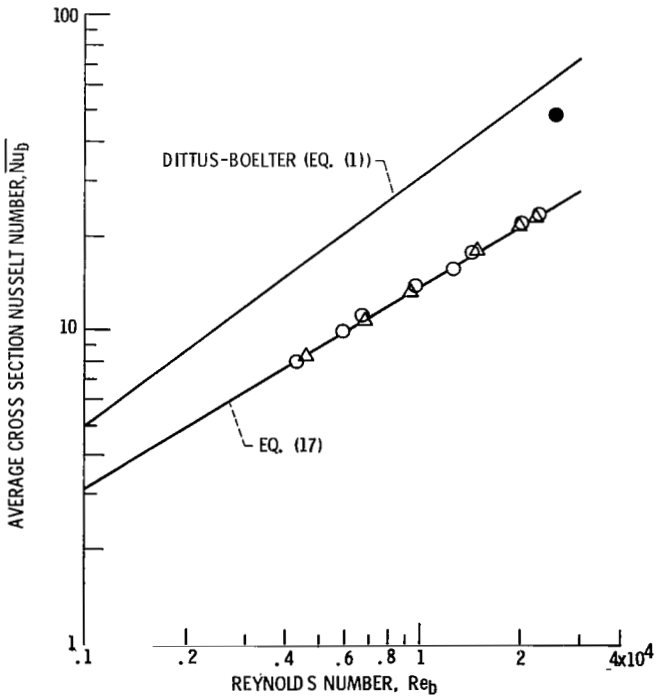

Figure 7. – Average cross section Nusselt numbers at exit section. Properties evaluated at local bulk temperature; $k_w t/kD_h = 24$; $x/D_h = 114$. (From ref. 32.)

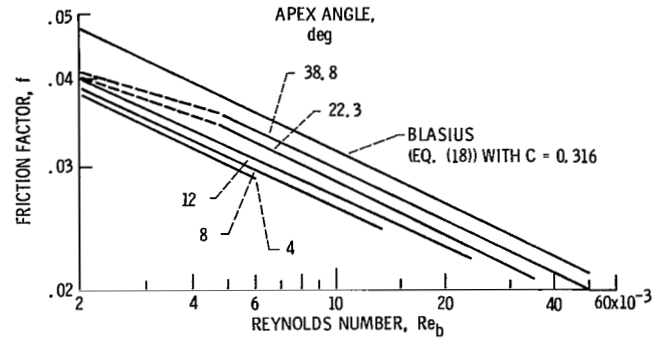

Figure 8. – Coefficient of friction for triangular ducts with small apex angles. (From ref. 33.)

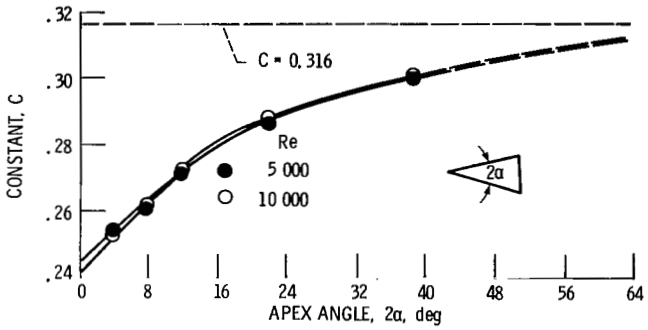

Figure 9. – Variation of the constant in the Blasius equation (eq. (18)) for friction as a function of the apex angle in a triangular duct. (From ref. 33.)

10°. At 27 diameters from the duct inlet, where the turbulent flow was fully turbulent and at Reynolds numbers of 5.7×10^5, the experimental data for the triangular duct agreed with Eckert and Irvine's correlation (ref. 32) to within 8 percent (fig. 10).

Altemani (ref. 35) studied the heat-transfer and pressure-drop characteristics of turbulent airflow in an asymmetrically heated, sharp-cornered, equilateral triangular duct. Two sides of the triangular duct were heated, and the third, unheated side made of low-conductivity material. Tests were conducted with negligible property variations with hydraulic-diameter-based Reynolds numbers from 4.0×10^3 to 6.0×10^4. The results (fig. 11) showed that the friction factors were 9 to 12 percent lower than either the Blasius equation or the Prandtl-Karman equation. The experimental data were found to fit best the correlation due to Malak, Hejna, and Schmid (ref. 36) given in the following equation:

$$\left(\frac{K_t}{f}\right)^{0.5} = 2 \log\left(\mathrm{Re}\, f^{0.5} K_t^{-1.5}\right) - 0.8 \tag{19}$$

where $K_t = 0.936$ for an equilateral triangular cross section.

For Reynolds numbers between 1×10^4 and 5×10^6, f can be approximated by the following equation:

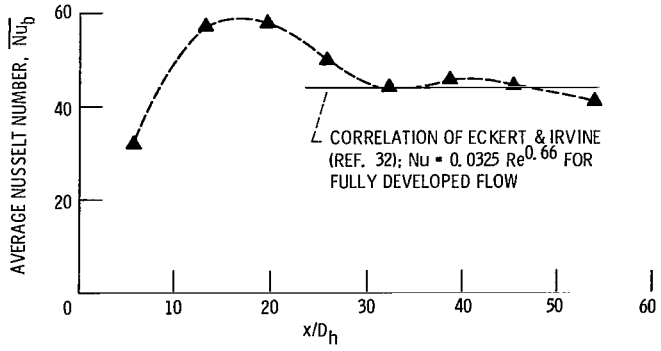

Figure 10. – Comparison of peripherally averaged Nusselt number for small-apex-angle triangular ducts. Short duration data; Reynolds number, 5.7×10^4. (From ref. 34.)

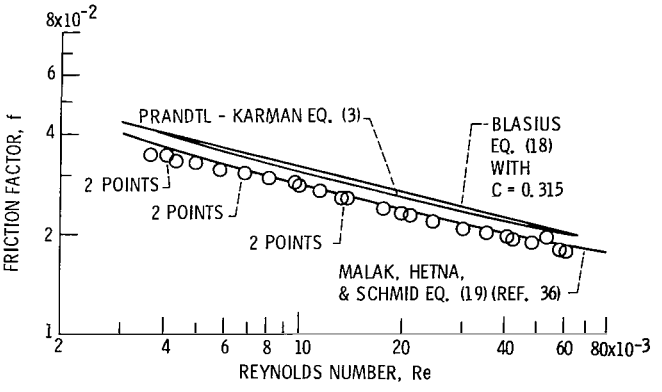

Figure 11. – Experimentally determined values of friction factor compared with correlations. (From ref. 35.)

$$f = (1.82 \log \mathrm{Re} - 1.64)^{-2} \qquad (20)$$

Figure 12 compares Altemani's experimental heat-transfer data with the Dittus-Boelter correlation (eq. (1)) and the Petukhov-Popov equation (eq. (2)). For Reynolds numbers between 1.0×10^4 to 6.0×10^4, the experimental heat-transfer data were about 15 to 22 percent lower than the Petukhov-Popov correlation and 27 to 30 percent lower than the Dittus-Boelter correlation. As discussed previously, the Eckert-Irvine correlation for a sharp cornered, isosceles triangular cross-section duct with a 11.46° apex angle was about 50 percent below the Dittus-Boelter correlation.

In an attempt to improve the correlation of the data and the Petukhov-Popov equation, Altemani used a measured friction factor in equation (2) instead of calculating it from equation (20) which was intended for a circular duct. With the substitution, he found that the experimental data correlated with equation (2) between 1 and 5 percent (fig. 13). He has suggested that this modification of the Petukhov-Popov equation could be used for Reynolds numbers from 1×10^4 to 5×10^6.

For pressure drop Hartnett, Koh, and McComas (ref. 37) presented a comprehensive comparison of predicted and measured friction factors for turbulent flow through

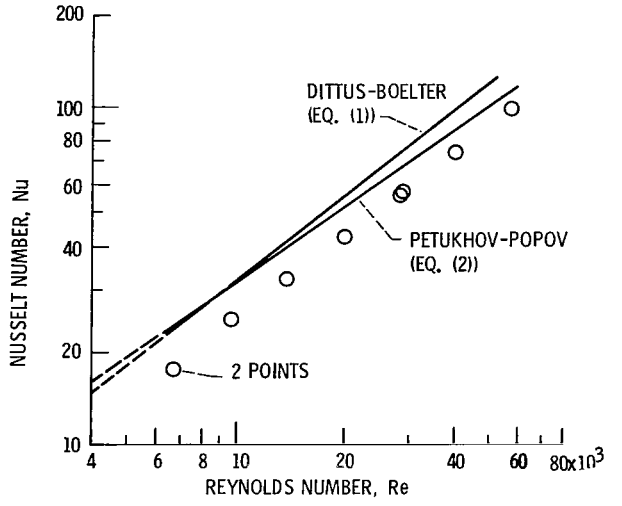

Figure 12. – Measured, fully developed values of the Nusselt number compared with Dittus-Boelter and Petukhov correlations. (From ref. 35.)

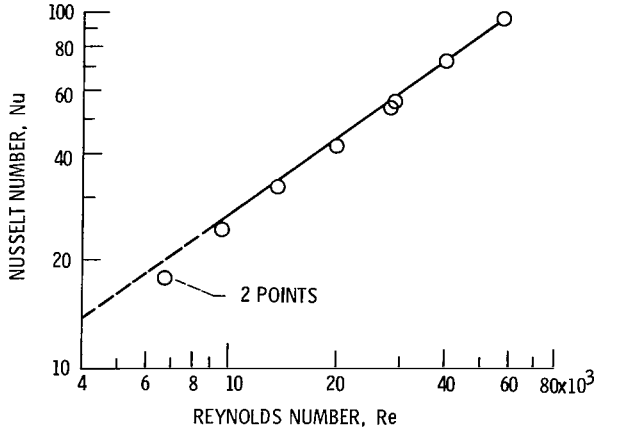

Figure 13. – Measured, fully developed values of the Nusselt number compared with the Petukhov-Popov equation (eq. (2)) modified by Altemani. (From ref. 35.)

rectangular ducts at ambient temperatures with no heat addition. Experimental data from other investigators (refs. 43 to 52), as well as from their own were used. They reported that for Reynolds numbers between 6×10^3 and 5×10^5, the circular tube correlation accurately represents the friction coefficient for flow through rectangular ducts for any and all aspect ratios (fig. 14). Examination of the figure shows that for the turbulent flow range, the agreement of most of the data is within 10 percent of the correlation.

Lowdermilk, Weiland, and Livingood (ref. 38) measured average heat-transfer coefficients and friction factors for air in turbulent flow at high heat fluxes for a square, a rectangle (aspect ratio = 5), and an equilateral triangle cross section. The surface temperatures ranged from 300 to 990 K (80° to 1320° F), and the Reynolds numbers ranged from 1×10^3 to 3.3×10^5. They reported that the average heat-transfer coefficients could be ap-

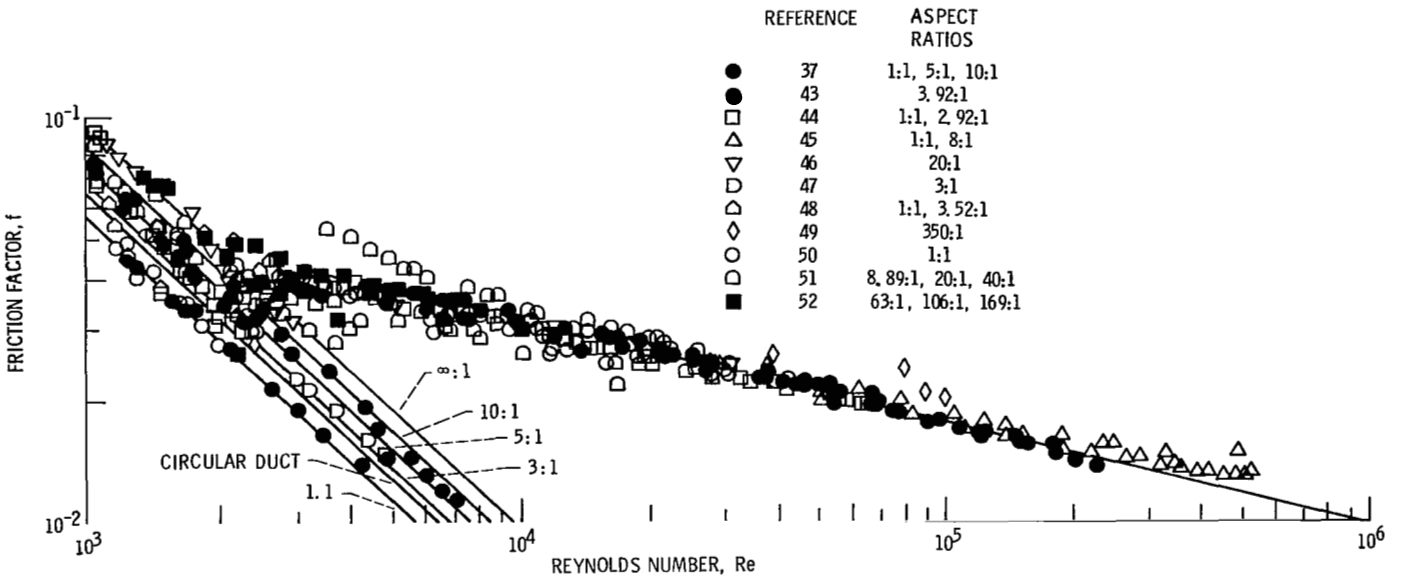

Figure 14. – Comparison of experimental friction factors for rectangular ducts with circular duct correlation. (From ref. 37.)

proximately correlated to circular duct results when the properties are calculated at the mean film temperature. Their experimental data were about 10 percent below the values predicted by the circular duct correlations with high heat fluxes in the turbulent regime (fig. 15). Attempts to correlate friction factors with the Karman-Nikuradse equation (eq. (3)) show only limited success (fig. 16 where the Karman-Nikuradse equation has been replotted as the Prandtl-Karman equation). The equation correlated the square duct data to within 20 percent (fig. 16(a)). The data for rectangular and trianglar ducts were as much as 35 percent higher than the Karman-Nikuradse equation.

Campbell and Perkins (ref. 39) investigated local friction factors and heat-transfer coefficients for turbulent airflow in a vertical, rounded corner, equilateral triangular duct. The local wall-to-fluid-bulk temperature ratios ranged from 1.1 to 2.1, with Reynolds numbers ranging from 1.09×10^4 to 3.7×10^4 at the inlet. Using bulk properties, a wall-to-bulk temperature ratio factor to account for the effect of variable properties, and an x/D_h factor to account for entrance effects, they arrived at the following correlation:

$$\mathrm{Nu}=0.021\ \mathrm{Re}^{0.8}\mathrm{Pr}^{0.4}\left(\frac{T_w}{T_b}\right)^{-0.7}\times\left[1+\left(\frac{x}{D_h}\right)^{-0.7}\left(\frac{T_w}{T_b}\right)^{0.7}\right] \qquad (21)$$

for $6.0<x/D_h<123$, $1.1<T_w/T_b<2.1$, and for properties evaluated at the bulk temperature. The experimental data were correlated to 15 percent and, with all but a few points, to within 10 percent (fig. 17). The authors noted that their heat-transfer coefficient was about 10 percent lower than the corresponding circular tube results of other investigators, but that the effect of T_w/T_b was about the same.

Campbell and Perkins also found that the ratio of friction factors based on both variable and constant properties can be correlated by the following equation for pressure drop, which included correction for entrance effects:

$$\frac{f}{f_{w,cp}}=\left(\frac{T_w}{T_b}\right)^{-0.4+(D_h/x)^{0.67}} \qquad (22)$$

for $14.5<x/D_h<72$; and $1.1<T_w/T_b<2.1$. The constant-property friction factor was found by using the modified wall Reynolds number as defined by

$$\mathrm{Re}_w^*=\frac{(D_hG)_b}{\mu_w}\frac{\rho_w}{\rho_b}$$

The authors claimed that the friction factors are extendable to x/D_h's from 5 to 200. They concluded that the friction factor for a rounded corner triangular duct is about 20 percent higher than the corresponding circular duct value for a T_w/T_b of 2.0.

Batista and Perkins (ref. 40) presented heat transfer and friction factors for turbulent airflow in a vertical square duct with moderate property variations, Reynolds numbers from 2.1×10^4 to 4.9×10^4, maximum wall-to-bulk temperature ratios to 2.13, and x/D_h's from 22 to 155. They found that the experimental heat-transfer data can be correlated by equation (21) (formulated by Campbell and Perkins for rounded corner triangular

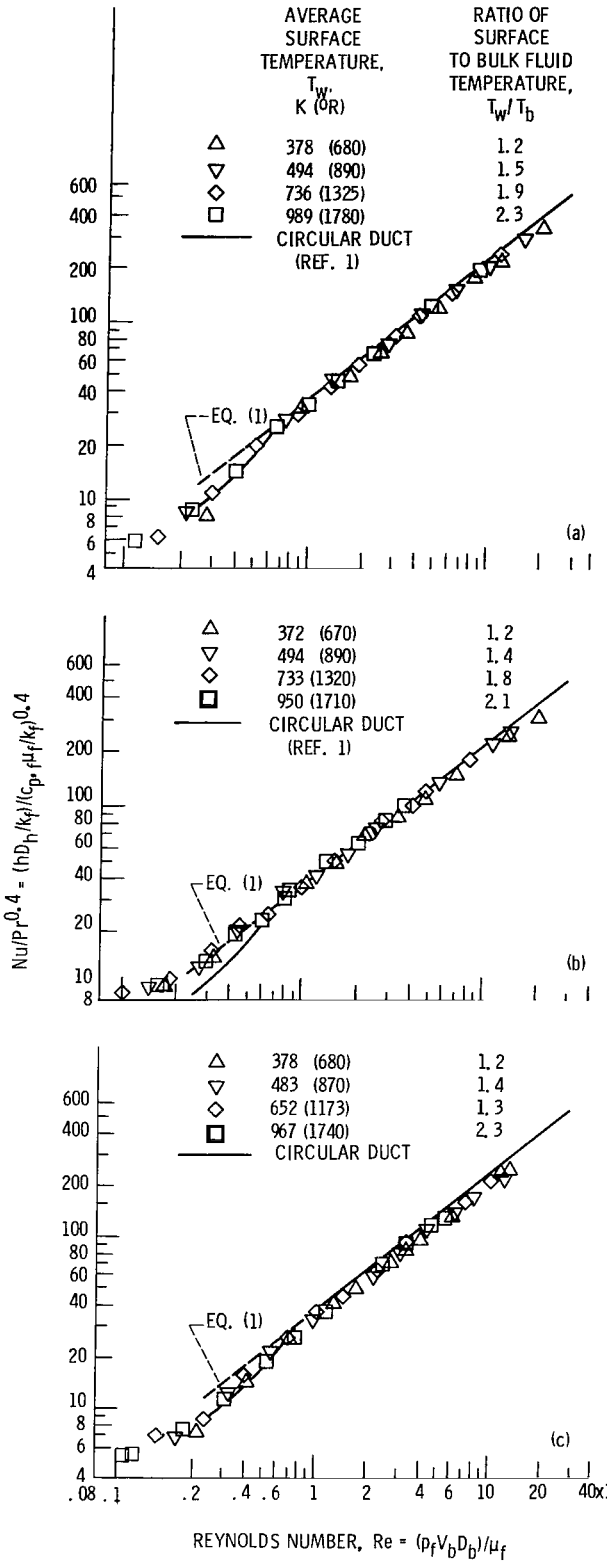

(a) Square duct.
(b) Rectangular duct.
(c) Triangular duct.

Figure 15. – Correlation of heat-transfer coefficients for airflow in ducts with variable heat flux. Bellmouth entrance; inlet temperature, 297 K (535° R); properties of air evaluated at film temperature. (From ref. 38.)

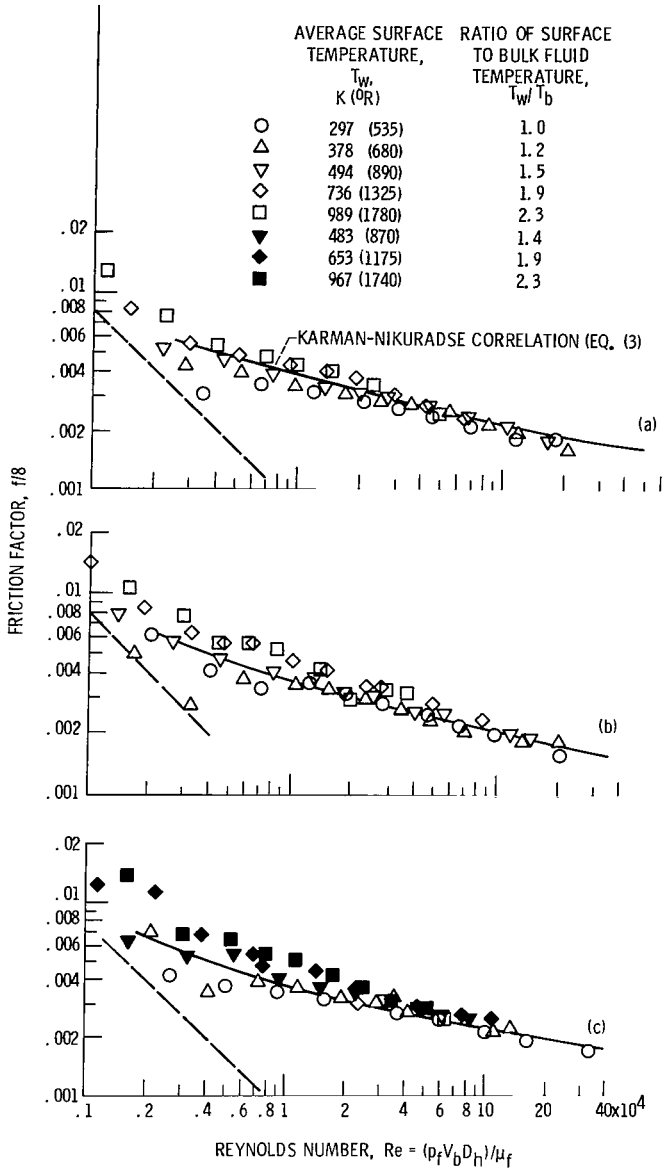

(a) Square duct.
(b) Rectangular duct.
(c) Triangular duct.

Figure 16. – Correlation of friction coefficients for airflow in ducts with variable heat flux (Prandtl-Karman correlation (eq. (3)). Viscosity and density evaluated at film temperature. (From ref. 38.)

ducts). (See fig. 18). The properties used are based on the bulk temperature. Figure 19 shows a correlation of friction factors for variable properties, normalized to constant property values and obtained at the same wall Reynolds numbers defined in the Symbols. Similar to Campbell's observations on heat transfer for rounded corner triangular ducts, Batista and Perkins (ref. 40) found that heat transfer to rounded corner square ducts was also about 10 percent below the circular duct results.

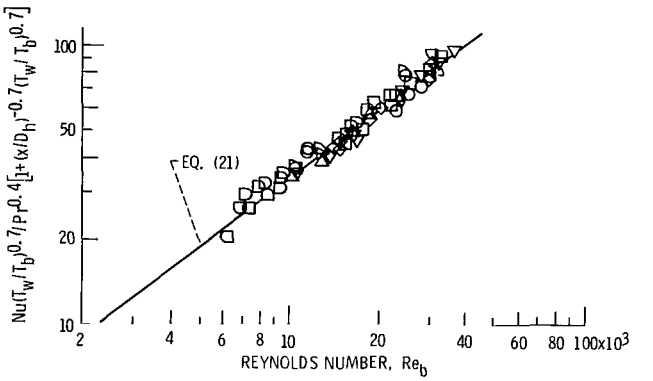

Figure 17. – Local heat-transfer results based on bulk properties. $6 < x/D_h < 125$; $1.1 < T_w/T_b < 2.11$. (From ref. 39.)

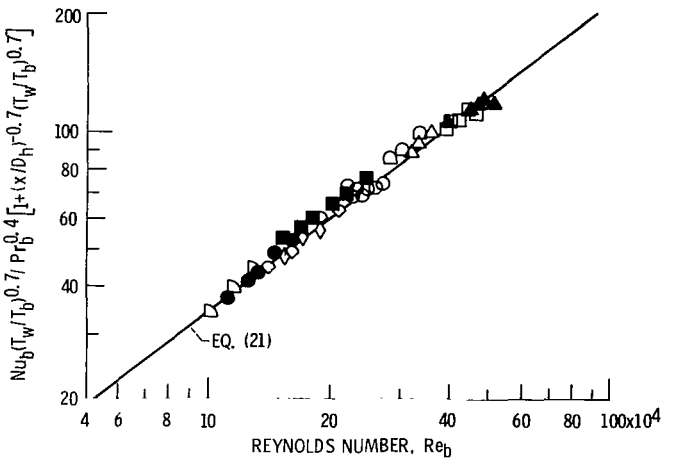

Figure 18. – Comparison of experimental heat transfer data of reference 40 with equation (21).

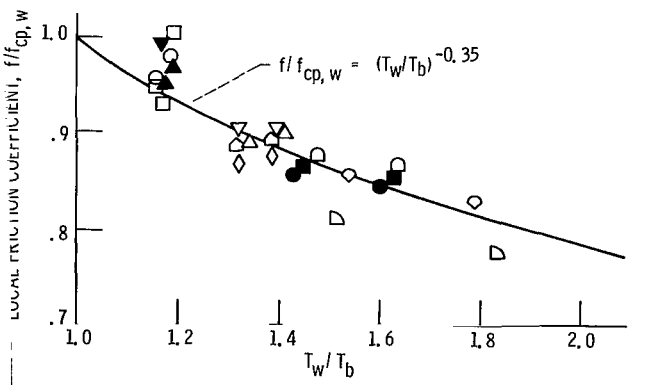

igure 19. – Local friction coefficients of reference 40 normalized to constant property values obtained at the same wall Reynolds number.

he friction factors for these geometries were about 20 ercent higher than those of the circular duct with the me heating conditions.

From the above discussion it is clear that numerous ublications are available for average heat-transfer and pressure-drop correlations for generally fully developed flow downstream of the inlet in both circular and noncircular passages. Generally, the correlations for average heat transfer are about ±10 percent. Because measurement accuracies in even fundamental experiments give a data scatter about a correlating equation of ±10 percent, the correlations for the circular tubes with fully developed flow and uniform heating are considered adequate, except for extreme geometries. However, more fundamental information on noncircular passages and peripheral heating variations may be suggested on which to base more accurate prediction methods or codes for these conditions. Such research, however, would be of low priority for advanced aircraft turbines because the coolant passage length-to-diameter ratios are relatively small in aircraft turbines, so that most of the passage length has developing flow rather than fully developed flow. The information discussed in the next section is probably of more direct need for most aircraft engine applications.

Entrance Region

Many of the correlations given in the previous section are only valid for heat transfer in fully developed turbulent flow. In turbine cooling applications the coolant generally travels through tortuous paths before abruptly entering the passages that will distribute the cooling air within the turbine blades or vanes. Within this entrance region hydraulic and thermal boundary layers generally develop simultaneously. The heat-transfer and flow characteristics in this entrance region differ from those in a fully established turbulent boundary layer. In advanced aircraft turbines with attendant low aspect ratio blades, non fully developed flow could occupy a considerable portion of the cooled passage length. For this reason this section was intended to specifically emphasize the entrance region of the flow passage.

Reynolds, Swearingen, and McEligot (ref. 54) presented an analytical method for predicting heat transfer at the thermal entrance region of a circular duct downstream of a fully developed hydrodynamic boundary layer. The solution, which used the method of Sparrow, Hallman, and Siegel (ref. 55), is based on a Reynolds-number-dependent velocity profile. Over a range of Reynolds numbers from 3.0×10^3 to 5.0×10^4, the predicted values lie within 5 percent of the experimental data. The authors of reference 54 showed that heat transfer to the thermal entrance region of a circular duct can be correlated to within 5 percent for entrance length-to-diameter ratios greater than 2.

Campbell and Slattery (ref. 57) presented an analytical approach for predicting the radial velocity and pressure profile downstream of the entrance of a circular tube with an assumed flat velocity profile. The results of their analysis as well as those of various investigators were compared with measurements of other investigators.

These comparisons showed that the predicted velocity profile development with downstream distance was reasonably good and that the predicted pressure-drop curve agreed to within 5 percent of the experimental data. Although the published literature (e.g., refs. 54 to 63) provide a better understanding of the physics of the flow and heat transfer at passage entrances, much of this research was performed under idealized conditions such as uniform velocities at the entrance and fully developed hydrodynamic boundary layers before heat addition and has little resemblance to entrances in turbine blades. A study by Boelter, Young, and Inerson (ref. 62) contains information that is probably of more immediate use to the turbine designer. Figure 20 (from ref. 62) shows the wide range of entrance geometries investigated, including bellmouths, gentle and sharp bends, long, short, and abrupt entrances. This array of entrance geometries, or slight variations of them, probably includes entrances of the types expected in turbine blades. The authors of reference 62 present plots of experimental local and average heat transfer coefficients for several values of turbulent flow Reynolds numbers as a function of distance from the entrance for each of the geometries shown in figure 20. Their results show that for some entrance geometries, the local heat-transfer coefficients at the entrance were as much as four times greater than the fully developed values in the downstream region. Altering the turbulence level ahead of most of the entrances (by the use of screens) had negligible effect on heat transfer for the conditions of their tests. The authors presented the following correlation for average heat-transfer coefficients for entrance tube lengths as a function of tube length to diameter ratios greater than 5.

$$\bar{h}=\bar{h}_{\infty}\left(1+K\frac{D}{x}\right) \tag{23}$$

where $\bar{h}$ is the average (circumferentially and axially)

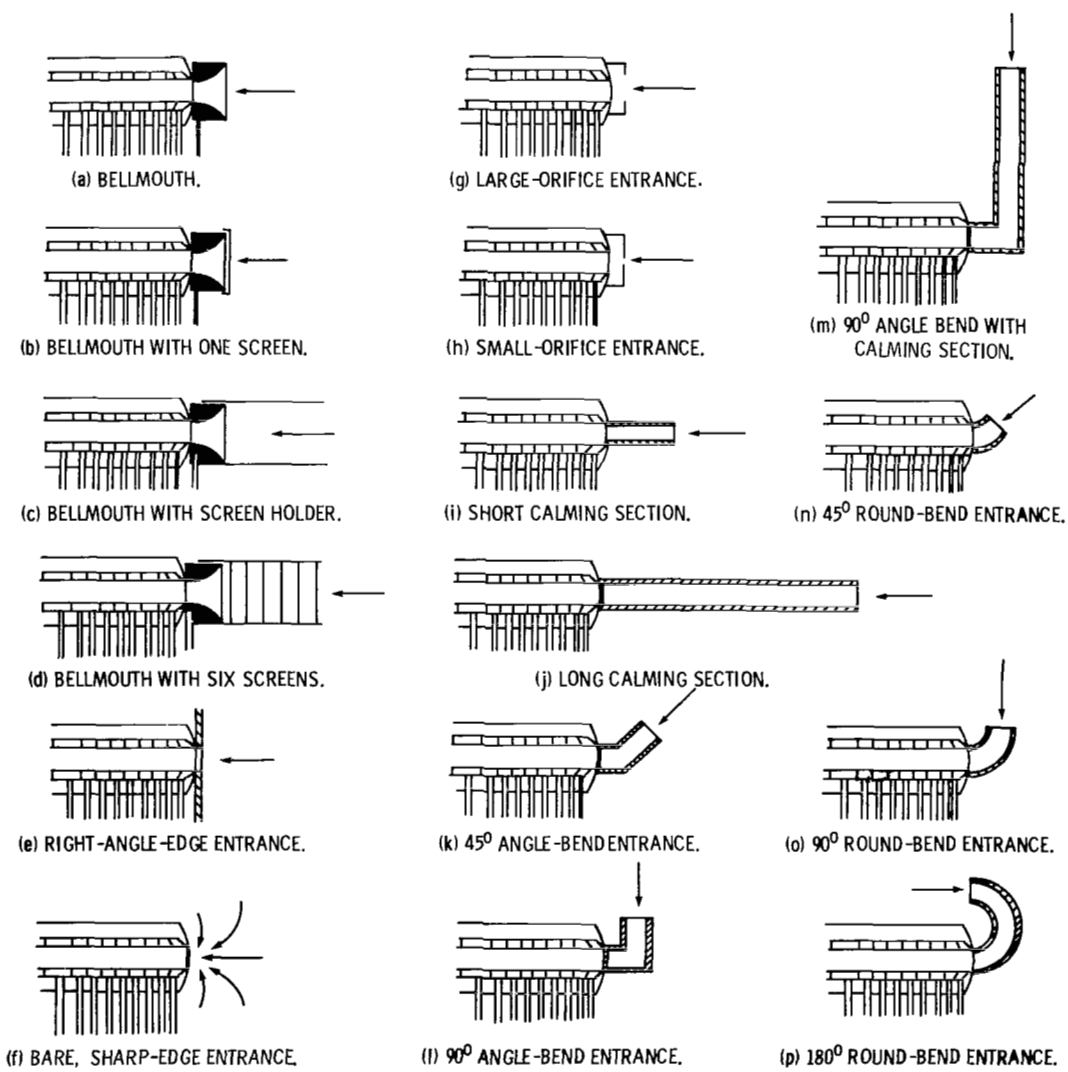

Figure 20. – Entrance conditions for which heat-transfer coefficients were determined by Boelter, et al., (ref. 62).

heat-transfer coefficient, $\bar{h}_\infty$ is the downstream average heat-transfer coefficient where both the hydraulic and thermal conditions are fully established, and K is the tabulated value (table I) for eight of the entrance geometries shown in figure 20. No correlation was given for the local heat-transfer values.

Since local heat-transfer values can be as much as four times greater than the fully developed downstream values, the effect on turbine metal temperature can be large. Further examination of the data of Boelter, Young, and Iverson (ref. 62) or additional data is needed to provide correlating equations for predicting local heat transfer coefficients as a function of distance from the inlet turbine blade and vane geometries.

Rotational Effects

At the high rotational speeds encountered in aircraft turbines, the Coriolis forces generate secondary flows within the flow channels. In addition, free-convection heat transfer becomes important because of the buoyancy forces caused by the density gradients and by the high centrifugal forces generated.

Several investigators have studied the phenomenon of combined free- and forced-convection heat transfer due to rotation. Some have experimented with liquids such as water as the working fluid. This review, however, is limited to investigations with air. Several investigators have approached the problem analytically. The equations generated in these analyses are best solved through the use of computer codes. Skiadaressis and Spalding (ref. 64) analyzed rectangular ducts, of aspect ratios (height/base) of 2:1, 1:1, and 1:2, rotating around an axis perpendicular to the ducts with radial coolant outflow and uniform heat flux through the duct walls. The authors indicated that for turbulent flow the heat-transfer and friction coefficients were increased by rotation and that heat transfer and flow were only weakly dependent on the aspect ratio. The increase in heat transfer between a passage with a 1:2 versus a 2:1 aspect ratio was about 10 percent. The analytical prediction showed a trend that agreed with the experimental data of Moore (ref. 69). Both references showed that on the pressure-side-wall (leeward side of rotation) heat transfer increased with rotation, whereas on the suction side wall heat transfer decreased with rotation. The end walls showed an increase with rotation. Moore's data showed these changes in heat transfer to be approximately 10 percent.

TABLE I. – CONSTANTS K FOR PREDICTIONS OF AVERAGE HEAT TRANSFER COEFFICIENTS FOR PASSAGES WITH GEOMETRIC ENTRANCES IN BOELTER, ET AL. (REF. 62)

Entrance conditions	K
Bellmouth (experimental)	0.7
Bellmouth with one screen:	
Ref. 62, Eq. (A4)	0.144 $Re^{0.25}$
Ref. 62, Eq. (A12)	1.1
Ref. 62, Eq. (A8)	0.128 $Re^{0.25}$
Experimental	1.2
Short calming section with sharp-edge entrance (experimental)	~3
Long calming section with sharp-edge entrance:	
Ref. 62, Eq. (A15)	0.067 $Re^{0.25}$
Experimental	1.4
45° angle-bend entrance (experimental)	~5
90° angle-bend entrance (experimental)	~7
2.5-cm (1-in.) square-edge-orifice entrance (experimental)	~16
3.8-cm (1½-in.) square-edge-orifice entrance (experimental)	~7

Mori, Fukada, and Nakayama (ref. 66) provided both analytical and experimental data on a straight circular pipe rotating around an axis perpendicular to its own with radial coolant outflow. The analytical results presented agreed reasonably well with the experimental data. The authors concluded that, in contrast to laminar flow, the local Nusselt number for fully developed turbulent flow had little variation in the circumferential direction, and that the increase in the Nusselt number over the nonrotating case was a little over 10 percent.

Lokai and Limanski (ref. 70) presented experimental heat-transfer data in radial channels of rotating turbine blades with radial coolant outflow. The rotational speed varied from 0 to 5000 rpm. The experimental data were correlated on the basis of similarity parameters. The data spread, however, is large. The correlation does not include the influence of a rotational Rayleigh number.

Ito and Nanbu (ref. 68) obtained extensive experimental data on velocity profiles and friction factors for fully developed laminar and turbulent flows in a circular pipe rotating about an axis perpendicular to its own with radial coolant outflow. They developed an empirical equation for friction factors. For turbulent flow the following equation for the ratio of friction factors with and without rotation (f/f_s) was shown to agree well (within 3 percent) with experimental data for values of a parameter K_t between 1 and 500:

$$\frac{f}{f_s} = 0.942 + 0.058\ K_t^{0.282} \tag{24}$$

where

$$K_t = \frac{Re_\Omega^2}{Re} = \frac{\Omega^2 D^4/\nu 2}{V_m D/\nu}$$

and where Ω is the angular velocity, V_m the mean axial velocity, D the pipe diameter, and ν the kinematic viscosity. For higher K_t values, the following equation may be used:

$$\frac{f}{f_s} = 0.924\, K_t^{1/20} \tag{25}$$

Skiadaressis and Spalding (ref. 64), in an analysis for a rotating circular tube with radial coolant outflow, obtained good agreement of their predicted velocity profiles and the experimental data of Ito and Nanbu (ref. 68). The analytical predictions of friction coefficients by Mori, Fukada, and Nakayama (ref. 66), however, showed better agreement with the experimental data of Trefethen (ref. 72).

Morris (ref. 67) analyzed and obtained experimental data on the rotational effect of a circular pipe rotating either parallel or perpendicular to the rotating axis. Experimental data were obtained for rotational speeds of up to 2000 rpm (approximately 1400 g's maximum at the midpoint of the pipe). Morris stated that, for a pipe rotating parallel to its axis, the Coriolis effects are more dominant in the entrance region and the rotational buoyancy effect is more important in the downstream developed flow region. Both these individual effects tend to improve heat transfer. For a pipe rotating perpendicular to its axis, the secondary flows generated by the Coriolis force generally help the heat-transfer process. However, the buoyancy effect on heat transfer may either be positive or negative, depending on the direction of flow. For radially inward flow the effect is positive; for radially outward flow the buoyancy force tends to offset and eventually reverse the increases in heat transfer brought about by the Coriolis interaction.

Morris and Ayhan (ref. 76) particularly stressed the possible overprediction in heat transfer which may result from the use of theoretically and experimentally derived equations that do not include the effect of buoyancy. Figure 21 shows that the average Nusselt number, relative to the nonrotating values, can very often be less than unity for the case of radially outward flow. Figure 21, which also compares the predicted results of other investigators (refs. 65, 66, 70, and 71), shows that the predicted values differ considerably among the investigators.

Morris and Ayhan (ref. 76) correlated experimental data such as shown in figure 21 for two test sections A and B. The range of test conditions is shown in table II. The resulting correlating equation for radially outward flow is given as follows:

$$\overline{\mathrm{Nu}} = 0.022\ \mathrm{Re}^{0.8}\left(\frac{\mathrm{Ra}_b}{\mathrm{Re}^2}\right)^{-0.186} S^{0.33} \tag{26}$$

where Re is the coolant flow Reynolds number, Ra is the rotational Rayleigh number (based on wall-bulk temperature difference), and S is the Rossby number.

A plot of Morris' and Ayhan's experimental data against this correlation for radially outward flow is shown in figure 22, where the mean scatter band for the

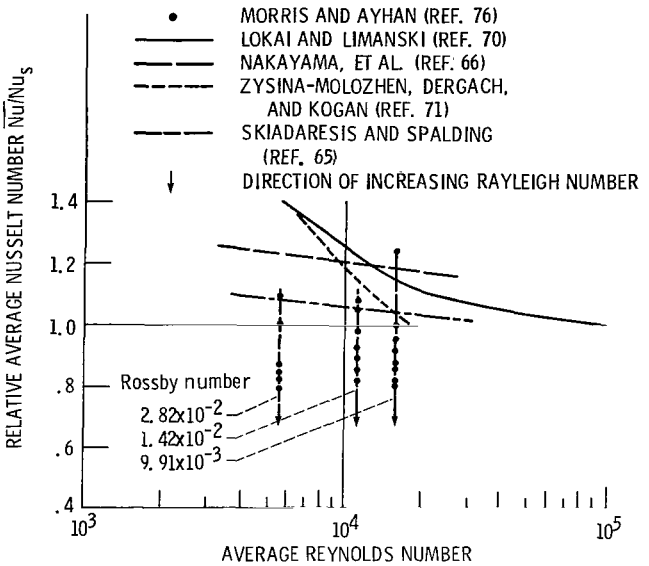

Figure 21. – Experimentally determined average Nusselt numbers (normalized to nonrotating values) for a tube rotating about its longitudinal axis for radially outward flow. Rotational speed, 1000 rpm. (From ref. 76.)

TABLE II. – NOMINAL RANGE OF VARIABLES COVERED IN EXPERIMENTS REPORTED IN REFERENCE 76

Test section	A	B
Length to diameter ratio	20.62	10.00
Eccentricity parameter	126.19	65.60
Nominal Reynolds number	5000 – 15 000	5000 – 15 000
Nominal Rossby number	1×10^{-2} – 6×10^{-2}	4×10^{-2} – 2.3×10^{-1}
Nominal rotational Rayleigh number	2×10^{-1} – 6×10^{5}	5×10^{5} – 9×10^{6}

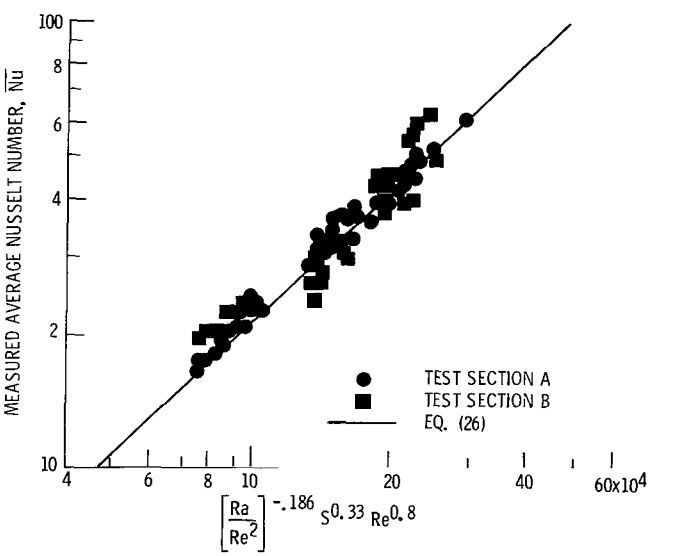

Figure 22. – Comparison of equation (26) with experimental data for radially outward flow. (From ref. 76.)

correlation is ±15 percent. They noted that extrapolations of the correlating equation to the conditions of industrial and aircraft gas turbine engines with radial coolant outflow show reductions of Nusselt numbers of 35 and 46 percent, respectively, compared with those predicted for nonrotating passages. They further speculate that this may explain why actual blade temperatures are higher than those predicted from nonrotating cascade tests.

Recently Morris (ref. 77) presented a comprehensive treatise on heat transfer in rotating channels which included many of his earlier works. Figure 23 (from ref. 77) showed a plot similar to that of figure 21, but for radially inward flow. The figure showed that for radially inward flow heat transfer is enhanced by rotation and increases with increasing Rayleigh numbers. Predicted values from other investigations (refs. 65, 66, 70, and 71) were compared as in figure 21. These investigations did not indicate a difference in the predicted heat-transfer values for inward and outward flow.

Reference 77 gave the following equation for radial inward flow, which is analogous to the radially outward flow equation (26):

$$\overline{Nu} = 0.036\ Re^{0.8}\left(\frac{Ra_b}{Re^2}\right)^{-0.112} S^{-0.083} \qquad (27)$$

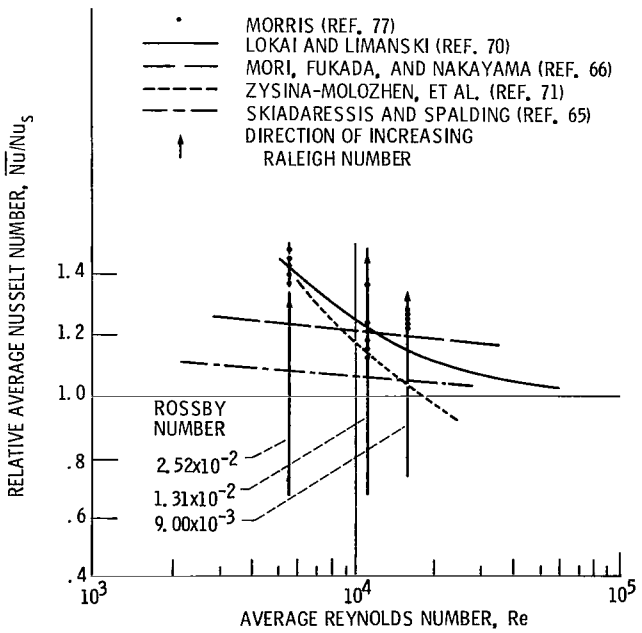

Figure 23. – Experimentally determined mean Nusselt numbers (normalized to nonrotating values) for tube rotating about its longitudinal axis for radially inward flow. Rotational speed, 1000 rpm. (From ref. 77.)

Figure 24 (from ref. 77) shows experimental data compared with equation (27). The stated mean scatter for this correlation is ±13 percent.

Although some excellent analytical work has been done and experimental data obtained at low centrifugal and buoyancy conditions, the effect of centrifugal and buoyancy forces at high heat flux and high rotational speeds still requires verification. These buoyancy forces can negate or augment the heat-transfer process in the cooled passages (ref. 77). Typical rotative speeds and acceleration levels for advanced, large turbine engines are of the order of 17 000 rpm and 75 000 g's and for small gas turbines, 65 000 rpm and 400 000 g's; whereas the experimental data obtained were for rotative speeds from 0 to 2000 rpm and a maximum acceleration level of 1400 g's. Although empirical correlations have been obtained for the average heat-transfer coefficient in a tube for both radial coolant outflow and inflow, further research is needed to expand the analytical predictive capabilities, to extend the experiment range to higher Rayleigh and Reynolds numbers, and to develop reliable, simplified correlations suitable for design purposes. In addition, since many coolant passage designs incorporate turbulators (discussed later) to increase the heat-transfer coefficients, the interaction of the effects of turbulators and rotation, particularly near the passage entrance and exit region, needs to be investigated. Research is also needed to determine the effect on heat transfer when the coolant passage is not radial to the axis of rotation, such as occurs at the leading and trailing edges of the airfoil.

Because local metal temperatures are important to turbine-blade life, research is also needed to obtain prediction methods and correlations for local heat-transfer

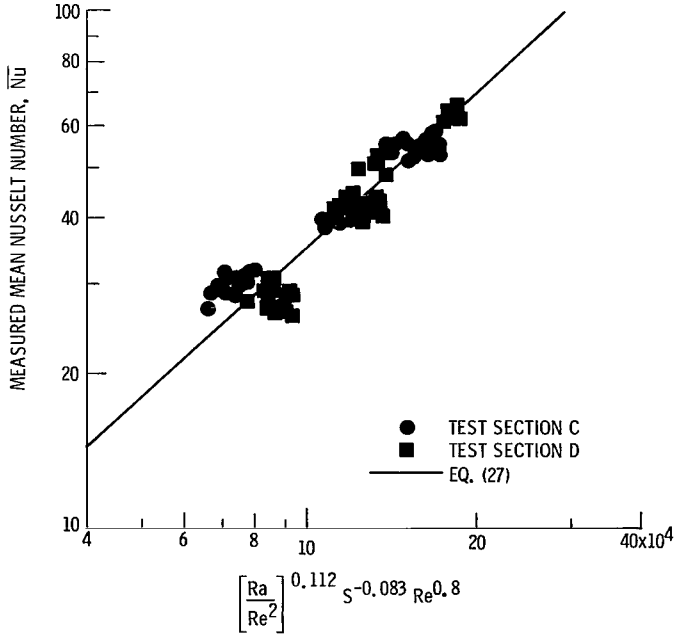

Figure 24. – Comparison of equation (27) with experimental data for radially inward flow.

coefficients along and around the rotating coolant passages, as well as for coolant pressure drops. Accurate experiments are needed to help develop the prediction methods and correlations.

Impingement

Experience has shown that, in advanced aircraft turbines, with attendant high gas temperatures and high pressures, simple convective cooling, if not combined with other forms of cooling, is not adequate to cool the blade material to an acceptable level. Impingement cooling is often used to cool the leading edge as well as the midchord areas.

Leading Edge

The leading-edge area in the airfoil is more difficult to cool than other areas because of the very high heat-transfer rates encountered in the gas stream at the stagnation area. Impingement cooling is often used to cool the leading edge. Figure 25 is a schematic sketch of an impingement cooled leading edge. Many investigators have studied single-row jet impingement on the inside of semicylindrical surfaces to model the leading edge of turbine blades (e.g., refs. 78 to 90).

Chupp, Helm, and McFadden (ref. 78) obtained experimental results on geometrical configurations and the range of variables that are representative in aircraft turbines. They reported that for Reynolds numbers bewteen 3.0×10^3 and 1.5×10^4, the following correlation for stagnation line heat transfer fits the experimental data to within 9 percent:

$$\mathrm{Nu}_0 = 0.44\ \mathrm{Re}^{0.7}\left(\frac{d}{c}\right)^{0.8} \times \exp\left[-0.85\left(\frac{z}{d}\right)\left(\frac{d}{c}\right)\left(\frac{d}{D}\right)^{0.4}\right] \quad (28)$$

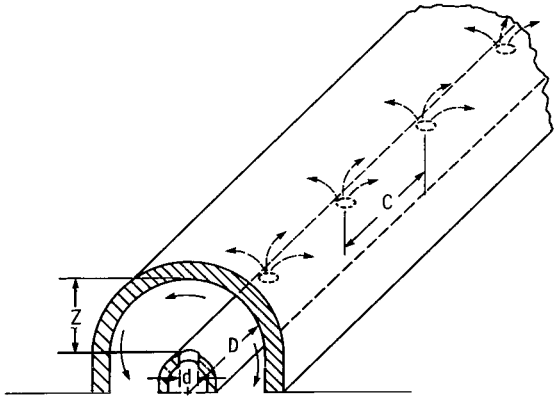

Figure 25. – Schematic of impingement-cooled leading edge.

where d is the jet hole diameter and D is the leading edge inside diameter. For average heat-transfer coefficient in the leading-edge area, the following correlation was reported to fit experimental data to within 8.7 percent:

$$\mathrm{Nu} = 0.63\ \mathrm{Re}^{0.7}\left(\frac{d}{c}\right)^{0.5}\left(\frac{d}{D}\right)^{0.6} \times \exp\left[-1.27\left(\frac{z}{d}\right)\left(\frac{d}{c}\right)^{0.5}\left(\frac{d}{D}\right)^{1.2}\right] \quad (29)$$

The local heat-transfer coefficients away from the stagnation line can be obtained from figure 26 (from ref. 78). It gives the normalized Nusselt number as a function of distance from the stagnation line, using the distance from jet nozzle to impingement target as a parameter.

References 79 to 81 represent some of the works by Metzger on leading-edge impingement cooling. Metzger, Yamashita, and Jenkins (ref. 80) reported that the maximum heat-transfer coefficient at the leading-edge area (obtained at optimum nozzle-to-target distance defined in ref. 80) is given as

$$\overline{\mathrm{St}} = \mathrm{Re}^{0.27}\left(\frac{l}{b}\right)^{0.52} = 0.355 \quad (30)$$

The heat-transfer coefficient is an average over an area l/b, where l is the arc length distance along the semicylinder from the stagnation line and b is the equivalent slot width. The authors reported that the above correlation holds for Reynolds numbers (based on equivalent slot width) from 1150 to 6300, and for spanwise hole spacing to diameter ratios c/d from 1.67 to 6.67. This correlation does not include the effect of any variation in the diameter of the target cylinder.

Damerow, et al., (ref. 82) determined the flow characteristic for rows of impingement holes in terms of discharge coefficients as a function of the jet-to-target

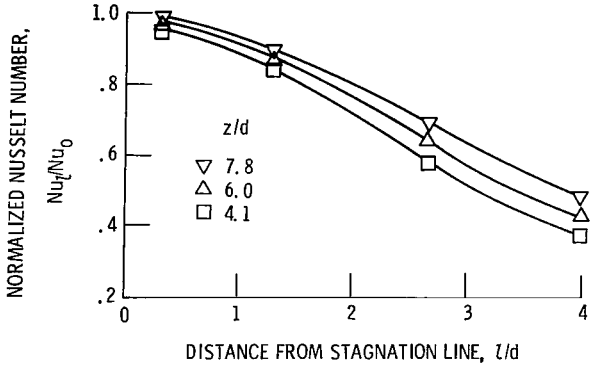

Figure 26. – Normalized Nusselt number as function of distance from stagnation line. Impingement hole diameter, 0.041 cm (0.016 in.); center-to-center distance between holes, 0.328 cm (0.125 in.); leading-edge inside diameter, 0.239 cm (0.094 in.).

spacing to the jet diameter ratio z/d, and coolant passage Mach number M. The equation which correlated the experimental data within about 15 percent was:

$$C_d = 0.819\left(\frac{z}{d}\right)^{0.045} M^{0.057} \tag{31}$$

where M is the coolant Mach number.

A total-pressure loss coefficient K_{tot} was also determined; the correlation of the data to within about 3 percent is a function of coolant Mach number and not influenced by the flow variations as the coolant is discharged through the impingement holes or by the impingement hole spacings. The correlation given is

$$K_{tot} = 0.97 + 0.465\ M^2 \tag{32}$$

and

$$\Delta P_{tot} = K_{tot}\frac{\rho v^2}{2}$$

The coefficients obtained were used in a compressible flow network computer code to predict the flow distribution in a simulated complex turbine-blade cooling design. The authors of reference 82 stated that the predictions compared favorably with experimental data (within 6 to 17 percent, depending on location).

In spite of the excellent work already done, there is still considerable variance among the correlations available in literature, as shown in figure 27 (from ref. 83). In this figure both the Reynolds and Nusselt numbers have been redefined using an equivalent slot width ($b = \pi d^2/4c$) as the characteristic length. Table III (also from ref. 83) shows the restated heat-transfer correlations using the equivalent slot width. There are also uncertainties in certain areas such as at the stagnation point that need to be investigated. Very little has been published on the effect of the shape of the leading-edge cavity (other than cylindrical) on heat-transfer coefficient. Only limited data are available on the use of multiple rows of holes. Additional data on local heat-transfer coefficients away from the stagnation line would be helpful. Additionally, the range of variables, including the range of impingement hole spacings and Reynolds numbers, needs to be extended.

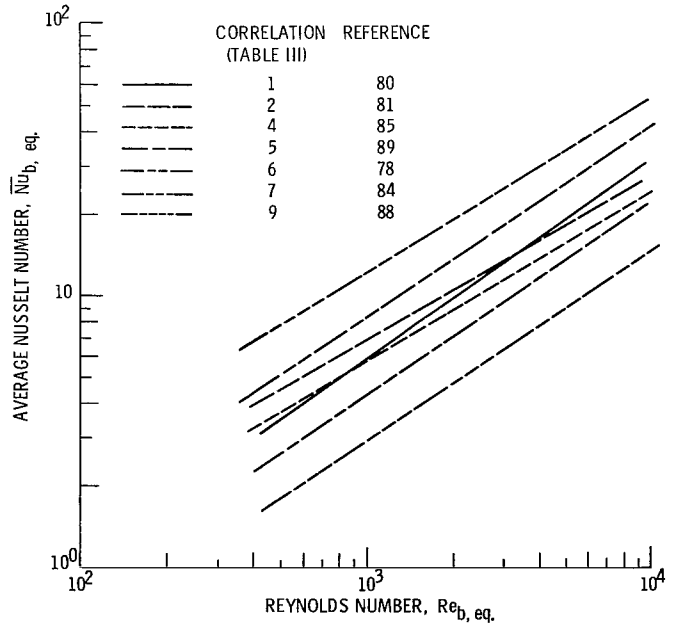

Figure 27. – Comparison of heat-transfer correlations for impingement into cavity using the equivalent slot width $b = \pi d^2/4c$ for both Nusselt and Reynolds numbers. (From ref. 83.)

More work is also needed for cases where the spent air is removed through bleed holes. In advanced aircraft turbines with high gas inlet temperatures and pressures, impingement cooling is often combined with film cooling. The spent air, instead of exiting at the open end of the channel, exits through film coolant holes in the blade leading edge to form a film of cooling air on the external surface for added protection to the blade metal.

Midchord

Impingement cooling at the midchord region usually uses rows of round holes. Here, the curvature of the blades is small so that jet impingement on flat plate correlations are generally used. Figure 28 is a schematic sketch of an impingement cooled flat plate. Fairly extensive literature is available for flat plate impingement cooling. References 91 to 110 are some representative publications.

Reference 91 is among the more frequently cited publications for jet impingement on flat plate. In these tests Kercher and Labakoff used a series of square arrays of round jets. The spent air is allowed to flow across the plate, creating a cross flow condition that is similar to those encountered in actual turbine-blade designs. The experimental data were correlated with the following relationship:

$$\mathrm{Nu} = \varphi_1\varphi_2 \mathrm{Re}^m \mathrm{Pr}^{1/3}\left(\frac{z}{d}\right)^{0.091} \tag{33}$$

where the Nusselt and Reynolds numbers are based on the jet impingement hole diameter, φ_1 and the power m are functions of impingement hole geometry and Reynolds number, and φ_2 is an attenuation factor to account for crossflow effects. Colladay (ref. 105) curve-fitted the experimental data and presented them in the following form:

$$m = a_1\left(\frac{x_n}{d}\right)^2 + b_1\left(\frac{x_n}{d}\right) + c_1 \tag{34}$$

TABLE III. – RESTATED HEAT TRANSFER CORRELATIONS FOR IMPINGEMENT INTO A CAVITY—USING EQUIVALENT SLOT WIDTH $b = \pi d^2/4c$ FOR BOTH NUSSELT AND REYNOLDS NUMBERS (FROM REF. 83)

$[D_h = 2bc(n-1)/[b + c(n-1)];\ D_{eff} = 4l/\pi]$

Correlation number	Correlation	Reference	Ratio of cylinder to nozzle diameter, D/d	Ratio of nozzle spacing to nozzle diameter, c/d	Ratio of nozzle to target separation distance to nozzle diameter, z/d	Ratio of nozzle to target separation distance to equivalent slot width, z/b	Ratio of cooled surface target length to equivalent slot width, l/b	Reynolds number, $Re_{b,eq}$
1	$Nu_{b,eq} = \frac{0.355}{2^{0.27}} Pr \left(\frac{b}{l}\right)^{0.52} Re_{b,eq}^{0.73}$	80	8.33	1.67 to 6.67	------	2 to 35	4.7 to 55.6	575 to 3150
2	$Nu_{b,eq} = 0.87\ Pr \left(\frac{b}{l}\right)^{0.475} \left(\frac{b}{D_h}\right)^{0.386} Re_{b,eq}^{0.614}$	81	8.33	1.67	------	1 to 15	1.6 to 14	875 to 3150
3	$Nu_{b,eq} = 0.2\ Pr \left(\frac{b}{l}\right)^{0.504} \left(\frac{b}{D_h}\right)^{0.208} Re_{b,eq}^{0.792}$	81	8.33	6.67	------	4 to 15	6.2 to 36.9	700 to 2500
4	$Nu_{b,eq} = 0.36 \left(\frac{b}{2l}\right)^{0.38} Re_{b,eq,a}^{0.62}$	85	3.6	3.3	1.8 to 7.3	15.5	12.2	2300 to 41 000
5	$Nu_{b,eq} = 0.8113 \left(\frac{d}{D_{eff}}\right)^{0.79} \left(\frac{d}{c}\right)^{0.126} \left(\frac{d}{z}\right)^{0.0135} \left(\frac{b}{2l}\right)^{0.285} Re_{b,eq}^{0.715}$	89	9.7 to 11.7	2.4 to 4.9	2 to 5.8	6 to 36.3	23.6 to 56.4	1800 to 41 000
6	$Nu_{b,eq} = 0.63 \left(\frac{b}{d}\right)^{0.3} \left(\frac{d}{c}\right)^{0.5} \left(\frac{d}{D}\right)^{0.6} \left\{\exp\left[-1.27 \left(\frac{z}{d}\right) \left(\frac{d}{c}\right)^{0.5} \left(\frac{d}{D}\right)^{1.2}\right]\right\} Re_{b,eq}^{0.7}$	78	1.54 to 15.6	4 to 15.6	1.0 to 16	0.35 to 700	20 to 180	300 to 2000
7	$Nu_{b,eq} = 0.03\ Pr^{1/3} \left(\frac{z}{b}\right)^{-0.4} Re_{b,eq}^{0.7} C_d^{-1}$	84	12.5	5	7.5 to 20	49 to 129	294	1000 to 6000
8	$Nu_{b,eq} = 0.26 \left(\frac{b}{D_h}\right)^{0.35} Re_{b,eq}^{0.65} \left(\frac{z}{b}\right)^{-0.22}$ for $\frac{z}{b} > 7$	88	------	------	------	7 to 13	7.3 to 12.2	2000 to 50 000
9	$Nu_{b,eq} = 0.17 \left(\frac{b}{D_h}\right)^{0.35} Re_{b,eq}^{0.65}$ for $\frac{z}{b} \geq 7$	88	------	------	------	1.5 to 7	2 to 7.3	2000 to 50 000

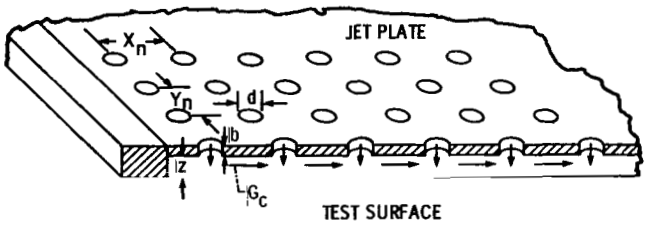

Figure 28. – Schematic of impingement-cooled flat plate.

$$\varphi_1 = \exp\left[a_2\left(\frac{x_n}{d}\right)^2 + b_2\left(\frac{x_n}{d}\right) + c_2\right] \tag{35}$$

$$\varphi_2 = \frac{1}{1 + a_3\psi^{b_3}} \tag{36}$$

where $\psi = (G_c/G_j)\,(z/d)$ and where the constants are given in table IV. The range of variables investigated were Reynolds number from 3×10^2 to 3×10^4, jet spacing from 3.1 to 12.5 diameters, and jet to target spacing from 1.0 to 4.8. Figure 29 shows a comparison of experimental data from reference 91 with predicted values obtained from equation (33).

More recently, Florschuetz, et al., (refs. 106 and 107) made a thorough investigation of jet impingement on a flat plate using both staggered and in-line jet arrays. The experimental variables varied from average jet Reynolds numbers of 5×10^3 to 5×10^4, with individual jet Reynolds numbers as low as 2.5×10^3 and as high as 7×10^7, jet spacing from 5 to 15 diameters in the streamwise direction and 4 to 8 diameters in the spanwise direction, hole diameters from 0.0635 to 0.762 cm (0.025 to 0.300 in.), and target to hole spacing ratios from 1 to 3. The conclusion of this investigation was that the in-line jet arrays yielded higher heat-transfer coefficients than

TABLE IV. – CORRELATION CONSTANTS FOR EQUATIONS (34) TO (36)[a]

[Impingement heat transfer on flat plate]

Coefficient	For Reynolds numbers of 300 to 3000	For Reynolds numbers of 3000 to 30 000
a_1	−0.0015	−0.0025
b_1	.0428	.0685
c_1	.5165	.5070
a_2	0.0126	0.0260
b_2	−.5106	−.8259
c_2	−.2057	.3985
a_3	0.4215	0.4696
b_3	.580	.965

[a]From ref. 105.

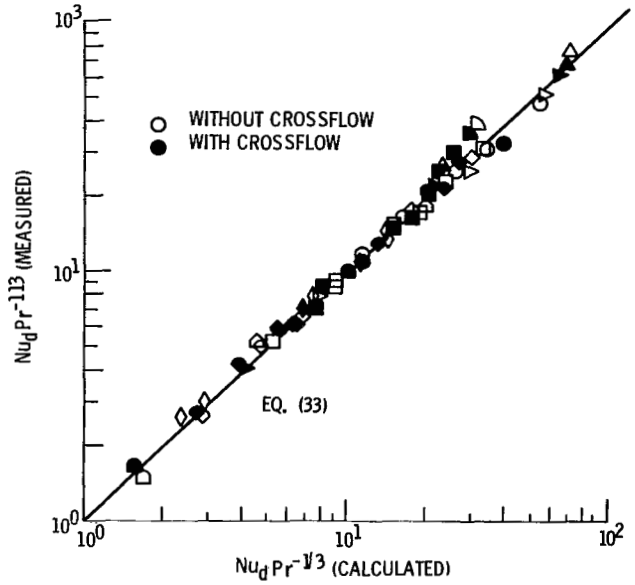

Figure 29. – Comparison of experimental data (ref. 91) and predicted Nusselt numbers.

the staggered configurations. At some point downstream of the point of injection, the degradation of impingement heat transfer is more than made up by the convective heat transfer.

As a result of this investigation, the authors recommend the following correlation for impingement heat transfer on a flat plate:

$$\mathrm{Nu} = \mathfrak{A}\,\mathrm{Re}_j^m\left[1 - \mathfrak{B}\,\frac{z}{d}\,\frac{G_c}{G_j}\right]^n \mathrm{Pr}^{1/3} \tag{37}$$

where Nu is the local Nusselt number in the streamwise direction, but averaged in the spanwise direction, and $\mathfrak{A}$, $\mathfrak{B}$, m, and n are each functions of geometry and take the following form:

$$\mathfrak{A},\ \mathfrak{B},\ m,\ n = C\left(\frac{x_n}{d}\right)^{nx}\left(\frac{y_n}{d}\right)^{ny}\left(\frac{z}{d}\right)^{nz} \tag{38}$$

The constants C, nx, ny, and nz, are each a function of $\mathfrak{A}$, $\mathfrak{B}$, m, and n, for both in-line and staggered arrays and are given in table V.

Out of 1400 data points for the in-line jet arrays, 95 percent fall within 11 percent of the fit line, and 99 percent fall within 16 percent of the fit line. For the staggered arrays with 680 data points, 95 percent of the points fall within 12 percent of the fit linend 99 percent of the points fall within 16 percent of the fit line.

In an alternative correlation, also from Florschuetz, et al., the exponents m and n are held constant. It is more convenient to use and is nearly as accurate as equation (37).

TABLE V. – CORRELATION CONSTANTS FOR EQUATION (38)[a]

[Impingement heat transfer on flat plate]

	Inline pattern				Staggered pattern			
	C	nx	ny	nz	C	nx	ny	nz
𝔄	1.18	−0.944	−0.642	0.169	1.87	−0.771	−0.999	−0.257
𝔪	.612	.059	.032	−.022	.571	.028	.092	.039
𝔅	.437	−.095	−.219	.275	1.03	−.243	−.307	.059
𝔫	.092	−.005	.599	1.04	.442	.098	−.003	.304

[a]From ref. 107.

$$\frac{\mathrm{Nu}}{\mathrm{Nu}_1} = 1 - C\left(\frac{x_n}{d}\right)^{nx}\left(\frac{y_n}{d}\right)^{ny}\left(\frac{z}{d}\right)^{nz}\left(\frac{G_c}{G_j}\right)^{n} \tag{39}$$

where Nu_1 is the Nusselt number for the first row of impingement jets (without the effect of crossflow) and is given as follows:

$$\mathrm{Nu}_1 = 0.383\left(\frac{x_n}{d}\right)^{-0.554}\left(\frac{y_n}{d}\right)^{-0.422} \times \left(\frac{z}{d}\right)^{0.068}\mathrm{Re}_j^{0.727}\mathrm{Pr}^{1/3} \tag{40}$$

The constants for equation (39) are given as follows:

	C	nx	ny	nz	n
Inline	0.596	−0.103	−0.380	0.803	0.561
Staggered	1.07	−.198	−.406	.788	.660

Figure 30 shows a comparison of equation (40) with the older correlation of references 91 and 97, for two square, in-line arrays, that fall within the the same range of test conditions. The agreement with reference 91 is good, but there is considerable variance with reference 97. This may be due to differences in the test geometry and test conditions, which were not clearly given in reference 97.

Damerow, Murtaugh, and Burggraf (ref. 82) obtained experimental data for discharge coefficients for impingement on a flat plate with crossflow. The data showed the effects of the variables of the tests to be insignificant, and the authors recommended a constant discharge coefficient of 0.78 as the best fit to the data. The spread in the discharge coefficients ranged between 0.7 to 0.9.

Florschuetz and Isoda (ref. 108) reported on the flow distribution and discharge coefficient effects for jet array impingement with initial crossflow. The authors reported that, for the geometries tested, the discharge coefficient remained essentially constant when there is no initial crossflow. With initial crossflow, the effect on the discharge coefficient is not significant if the ratio of initial

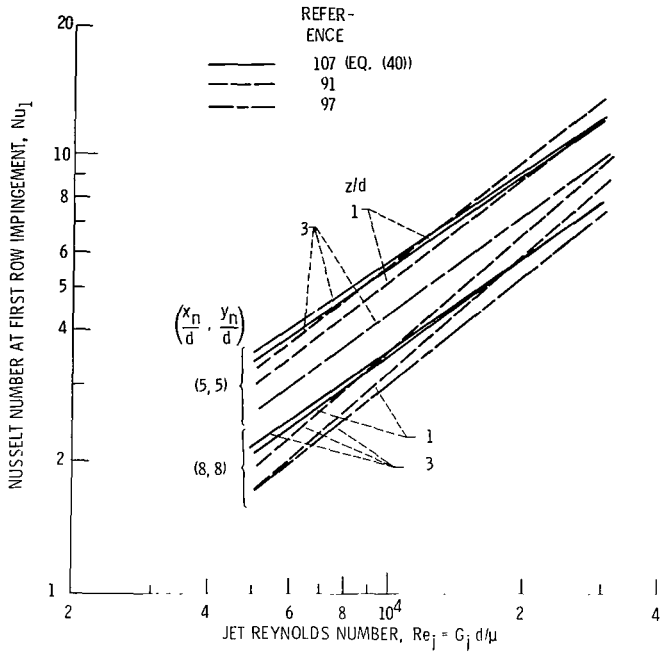

Figure 30. – Comparison of equation (40) for first row of impingement jet on flat plate with references 91 and 97 for two square, in-line jet arrays. (From ref. 107.)

crossflow to total jet flow $(G_c/G_j) \geq 1$, and the parameter $(y_n/d)\,(z/d) \geq 12$.

This discharge coefficient decreases as $(y_n/d)\,(z/d)$ decreases. The results of their experimental data are curve-fitted and presented in algebraic form in table VI. The function $\zeta(G_c/G_j)$ appearing in table VI is defined as follows:

$$C_d = \zeta(G_c/G_j) = \frac{1.06}{(G_c/G_j + 0.806)^{0.0602}} \tag{41}$$

Florschuetz and Isoda also presented a flow model to calculate G_c/G_j. For constant discharge coefficient C_d and for negligible friction $(f=0)$, G_c/G_j can be expressed as

$$\frac{G_c}{G_j} = \frac{1}{2C_d}\,\frac{(1+M)\sinh B\tilde{x} - M\sinh(1-\tilde{x}')}{(1+M)\cosh B\tilde{x} - M\cosh B(1-\tilde{x})} \tag{42}$$

where $B = \sqrt{2A_0^* C_d L/z}$, $\tilde{x} = x/L$, $\tilde{x}' = \tilde{x} - (1/2)(x_n/L)$, and $M = W_c/W_j$, the ratio of initial crossflow to total jet flow.

When discharge coefficient C_d is not constant or when f is not equal to zero, or both, the more general equation given in reference 108 must be solved numerically to obtain G_c/G_j using an equation and boundary conditions also given in reference 108.

Similar to impingement cooling of the leading-edge area, the midchord region can use film cooling in conjunction with impingement cooling. The spent air from impingement would exit through the film cooling holes.

TABLE VI. – DISCHARGE COEFFICIENTS FOR IN-LINE JET ARRAYS WITH CONFINED COOLANT DISCHARGE IN ONE-DIRECTION[a]

Configuration x_n/d, y_n/d, z/d	Equation (b)	Range of G_c/G_j
(5,4,1)	$C_d = \frac{0.85}{\zeta(G_c/G_j)}$	0 to 0.63 >0.63
(5,4,2)	$C_d = \frac{0.85}{1.08\ \zeta(G_c/G_j)}$	0 to 0.83 >0.83
(5,4,3)	$C_d = \frac{0.85}{1.11\ \zeta(G_c/G_j)}$	0 to 0.90 >0.90
(5,8,1)	$C_d = \frac{0.80}{-0.169\ (G_c/G_j)+0.893\ \zeta(G_c/G_j)}$	0 to 0.54 0.54 to 1.5 >1.5
(10,4,1) and (10,8,1)	$C_d = \frac{0.76}{-0.128(G_c/G_j)+0.825\ \zeta(G_c/G_j)}$	[c]0 to 0.54 [c]0.54 to 1.8 [c]>1.8

[a]From ref. 108.

[b]$\zeta(G_c/G_j)$ defined by eq. (41).

[c]Inferred from test data.

Hollworth, et al., (refs. 102 and 103) investigated jet impingement on a flat plate with vent holes on the target plate. The vent holes are placed either in-line with respect to the impingement jets or in a staggered geometry with respect to the impingement holes. The experimental data indicated that for the staggered-hole geometry, venting spent air through film cooling holes consistently yield higher heat-transfer rates (about 20 to 30 percent higher) than do the same arrays with edge venting of the spent air to one side (fig. 31).

In view of the growing use of film-cooling in conjunction with impingement cooling, additional research is needed in coupling these two cooling methods. Other areas that need attention are the determination of the significance of the effects of airfoil curvature and real turbine wall-to-coolant temperature ratios on correlations currently available. Research is also needed to determine the two dimensional heat transfer over the impinged surface because of the concern over possible large temperature gradients in the wall.

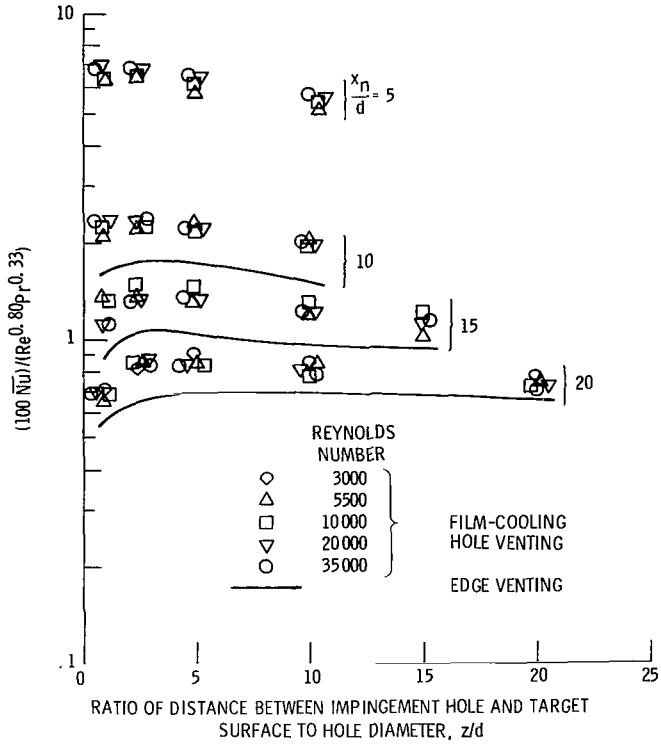

Figure 31. – Comparison of impingement heat transfer with staggered hole arrays: film-cooling-hole venting versus edge venting. (From ref. 102.)

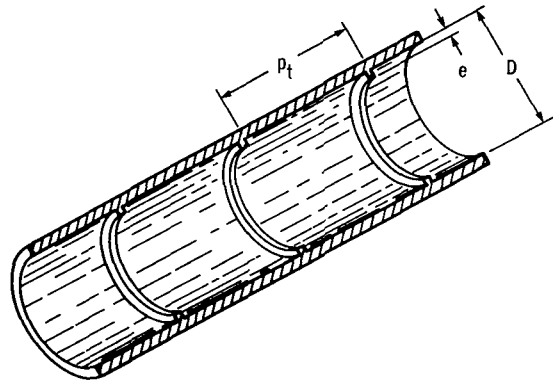

Figure 32. – Characteristic dimensions of typical turbulater design. Relative rib spacing, p_t/D.

Heat-Transfer Enhancement

Turbulators

The use of artificially roughened surfaces in the form of repeated ribs, or turbulators (fig. 32), has gained interest in recent years as a means of increasing heat transfer in the coolant passages of airfoils. The purpose of these ribs is to break up the boundary layer and thereby reduce the resistance to heat flow. This increase in heat transfer is, of course, also accompanied by an increase in pressure loss. Several publications have appeared in literature (refs. 111 to 118), and a few of them have direct application to turbine airfoil design. Webb (ref. 112) reported repeated ribs inside a circular tube and indicated that the optimum heat transfer occurs at a pitch-to-rib-height ratio of about 10.

For heat transfer, Webb gives the following correlation for Stanton number:

$$\mathrm{St}=\frac{f/2}{1+\sqrt{f/2}\left[\bar{g}\{e+\}\mathrm{Pr}^{0.57}-u_e^+\{e+,p_t/e\}\right]} \tag{43}$$

and friction factor f from

$$\sqrt{\frac{2}{f}}=2.5\ln\left(\frac{D}{2e}\right)+u_e^+\{e+\}-3.75 \tag{44}$$

Figures 33 and 34 show the heat-transfer and pressure-drop experimental data and suggested correlations taken from reference 112. Examination of the figures showed that the data are correlated to within a range of 10 to 20 percent. Webb, et al., correlated the data in figure 33 with the following equation:

$$\bar{g}=4.50(e+)^{0.28} \tag{45}$$

The authors further stated that by using $D_{eq}\equiv D-e$ in the f and Re calculations, the data scatter in figure 34 is

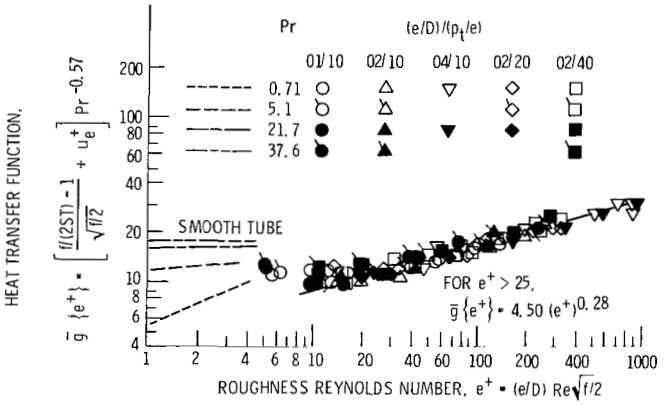

Figure 33. – Heat-transfer correlation for repeated ribs inside circular tubes. For $e^+>25$, $ge^+=4.50\ (e^+)^{0.28}$. (From ref. 112.)

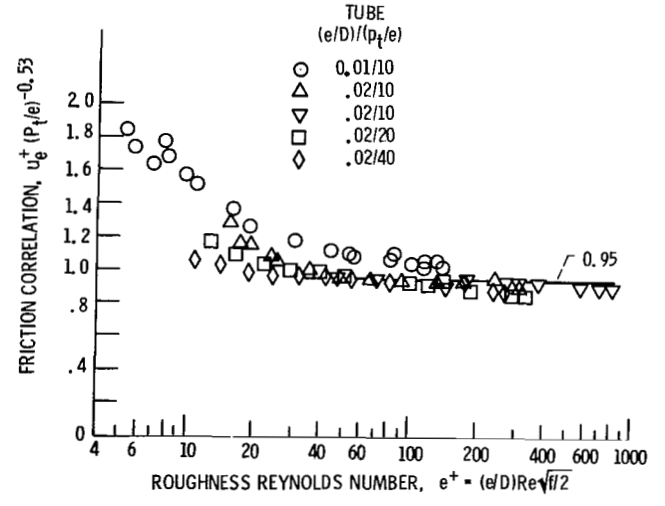

Figure 34. – Friction correlation (eq. (47)) for repeated ribs inside circular tubes. (From ref. 112.)

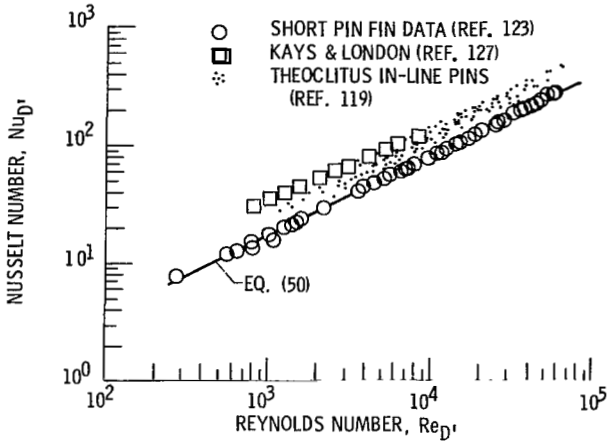

Figure 35. – Comparison of short pin fin data with long pin data. (From ref. 123.)

reduced to ±6 percent. The authors recommended a procedure for solving the pressure-drop and heat-transfer coefficients that requires using e^+ as an independent flow variable. This procedure requires the computation of St, f, and Re for several values of e^+ and then draw a curve of St and f versus Re. In the fully turbulent region ($e+>35$) and for $10<p_t/e<40$, the St and f can be calculated from the following equations (ref. 112):

$$\mathrm{St}=\frac{f/2}{1+\sqrt{f/2}\left[4.5(e+)^{0.28}\mathrm{Pr}^{0.57}-0.95(p_t/e)^{0.53}\right]} \tag{46}$$

and

$$\sqrt{\frac{2}{f}}=2.5\ln\left(\frac{D}{2e}\right)-3.75+0.95\left(\frac{p_t}{e}\right)^{0.53} \tag{47}$$

Han, Glickman, and Rohsenow (ref. 113) studied repeated ribs between parallel plates and determined the effects of rib shape, angle of attack, and pitch to height ratio on friction factor and heat transfer. For heat transfer, they give the following correlation:

$$g=\frac{10(e+/35)^i}{(\delta/45°)^j} \tag{48}$$

where

$i=0$ when $e+<35$; $i=0.28$ when $e+\geq 35$

$j=0.5$ when $\delta<45°$; $j=-0.45$ when $\delta\geq 45°$

For pressure drop, the following correlation is given:

$$u+=\frac{4.9(e+/35)^m}{(\theta/90°)^{0.35}[10/(p_t/e)]^n(\delta/45°)^{0.57}} \tag{49}$$

where

$m = -0.4$ if $e^+ < 35$; $m = 0$ if $e^+ \geq 35$

$n = -0.13$ if $p_t/e < 10$; $n = 0.53(\delta/90°)$ if $p_t/e \geq 10$

When δ and θ are both equal to 90°, $e^+ \geq 35$, and $p_t/e > 10$, this pressure-drop correlation is equivalent to the one given in reference 112 (eq. (47) herein), with the exception that the constant is changed from 0.97 to 0.95.

In view of the increasing usage of the repeated rib, additional work is required to determine the effects of rib orientations, geometry, noncircular passages, and passage rotation, with particular emphasis on local heat-transfer coefficients. Also, because the coolant passages with rib turbulators generally make several radial passes within the arifoil, reversing flow direction from pass to pass, the entrance effect and the turning effect are greatly magnified. Unpublished data showed that heat transfer coefficients increase by about a factor of 2 at locations downstream of the tightly curved returns. Additional research in this area is also needed.

Pins

Pins are frequently used in the trailing-edge region in turbine airfoil design. In figure 1 the chordwise ribs at the trailing edge are frequently replaced by pins. In such applications the pin height to the pin diameter ratio is not large ($l/d < 3$). These pins cannot be considered as extended surfaces because they often cover up more surface on the end walls than they provide. The primary purposes for using these pins are (1) to add rigidity to the trailing-edge surface, and (2) to act as turbulators, thereby increasing the heat transfer. But, as with any turbulence generator that increases heat transfer, they also increase pressure drop.

Numerous publications have appeared on pins as extended surfaces or as tubes in cross flow (refs. 119 to 127). They are also topics in any standard heat-transfer text book (e.g., refs. 28 and 29). Theoclitus (ref. 119) reported on heat transfer and pressure drop on many configurations of long tube bundles, mainly intended for heat exchanger usage and are of much larger h/d ratios than are of interest for turbine applications. Faulkner (ref. 121) presented a correlation for triangular pitched pins, but only from available experimental data, for longer l/d ratios. Recently, a few studies have treated short pins as applied to turbine-blade design (refs. 123 to 126). Van Fossen (ref. 123) reported on heat-transfer characteristics on short pins with equilateral triangular pitch. Such pins are representative of those used in turbine-blade cooling design. Van Fossen suggested the following correlation which agreed well with experimental data:

$$\mathrm{Nu} = 0.153\ \mathrm{Re}^{0.685} \tag{50}$$

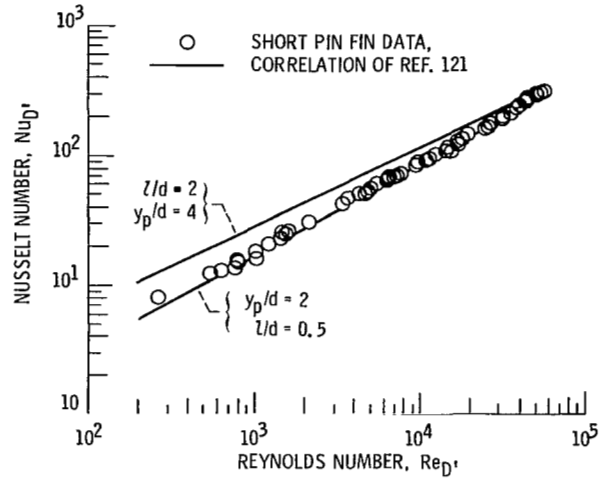

Figure 36. – Comparison of long pin fin heat transfer correlation (eq. (54)) with short pin fin data. (From ref. 123.)

The Reynolds number was defined as

$$\mathrm{Re} = \frac{(W/\bar{A})D'}{\mu} \tag{51}$$

where D' is the characteristic length ($=4v/S$) and $\bar{A}$ is the average flow area through the pin array section ($\bar{A} = v/L$). Properties were evaluated at the Eckert reference temperature:

$$T_r = 0.5\ T_w + 0.28\ T_s + 0.22\ T_{aw} \tag{52}$$

The adiabatic wall temperature used in the above equations was calculated as follows:

$$T_{aw} = T_s + R(T_{\mathrm{tot}} - T_s) \tag{53}$$

where R is the recovery factor ($=\sqrt{\mathrm{Pr}}$). Figure 35 compares equation (50) with experimental data from reference 123 for short fins and with the experimental data for pin fins obtained by two other investigators. The heat-transfer data for the short fins fall considerably below those for the long fins. Figure 36 compares experimental data of Van Fossen (ref. 123) with the Faulkner's correlation, given below (ref. 121):

$$\frac{hD'}{k_f} = \left\{0.023 + 4.143\ \exp\left[-3.094(d/p_p)\right.\right.$$

$$\left.\left. - 0.89(p_p/l)^{0.5075}\right]/\mathrm{Re}^{0.2946}\right\}\mathrm{Re}^{0.8}\mathrm{Pr}^{1/3} \tag{54}$$

where

$$\mathrm{Re} = \frac{D' G_{\min}}{\mu_f}$$

and

$$D' = \frac{4 A_{\min} L}{S}$$

The Faulkner correlation gives fairly acceptable values at high Reynolds numbers, but varies considerably at lower Reynolds numbers.

Van Fossen cautions that the good correlation obtained from equation (50) may be fortuitous because the correlation was obtained from only two different geometries of pin configurations and the pin arrays were limited to equilateral triangular arrangements. There were no pressure-drop data reported in reference 123.

Simoneau and Van Fossen (ref. 124) studied a single heated cylinder within an array of pins from one to six rows. A pin geometry of $l/d = 3.01$ for both in-line and staggered arrays was used. The authors concluded that the addition of pin arrays upstream in an in-line pattern of one to five rows produced an average 50 percent increase in heat-transfer level above the base case. For the staggered array, the average heat transfer increased by 21, 64, 58, 46, and 46 percent, respectively, above the base case for one to five rows of pins upstream.

Metzger and Haley (ref. 125) reported experimental results using two sets of short pins with the following geometry:

Set	x_p/d	y_p/d	l/d	d, cm	Streamwise rows
1	2.5	2.5	1.0	0.508	10
2	1.5	2.5	1.0	0.846	10

A duplicate set of pin arrays for each of the above geometries, but with pins made of nonconducting material, was also used in the experiments. The heat-transfer coefficient increased rapidly for the first few rows, with a higher peak row heat transfer in the closer streamwise spaced array, and decreased in the downstream rows. They also found that nonconducting pin heat-transfer results, averaged over the 10 row array, followed the conducting pin heat-transfer results closely, although with a slight difference in Reynolds number dependence. In all cases the average array heat transfer was significantly lower than would be predicted from the larger l/d (tube bank) correlations. For design purposes, the authors curve-fitted the experimental data and obtained the following correlations: For $x_p/d = 1.5$

$$\overline{\mathrm{Nu}} = 0.092\ \overline{\mathrm{Re}}^{0.707} \tag{55}$$

For $x_p/d = 2.5$

$$\overline{\mathrm{Nu}} = 0.069\ \overline{\mathrm{Re}}^{0.728} \tag{56}$$

where $\overline{\mathrm{Nu}}$ and $\overline{\mathrm{Re}}$ are the averages of the local Nusselt and Reynolds numbers for each individual pin row in the streamwise direction. Fluid properties for each local Nusselt number are evaluated at the arithmetic average between the local fluid bulk and the metal end wall temperatures, and the Reynolds number is based on maximum velocity and pin diameter.

Figures 37 and 38 (from ref. 125) show the experimental Nusselt numbers plotted against equations (55) and (56), respectively. Van Fossen replotted the data (from figs. 37 and 38) using Reynolds number as defined in equation (51). The resulting plot was well correlated by equation (50), as seen in figure 39.

Additional work on short pins is needed. Equations (50), (55), and (56) are for specific pin array geometries. Heat-transfer data are needed on other pin configurations and pin arrays to formulate a more general correlation. Data on presssure drop is particularly needed since little or no published data exist for short pins.

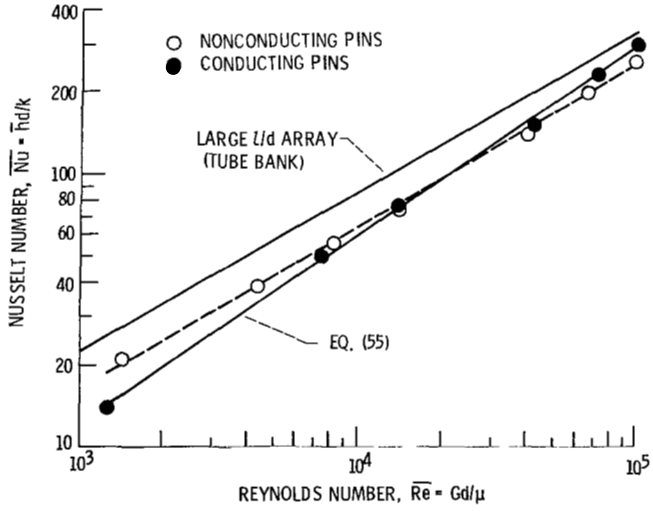

Figure 37.—Nusselt number as function of Reynolds number for $x_p/d = 1.5$. (From ref. 125.)

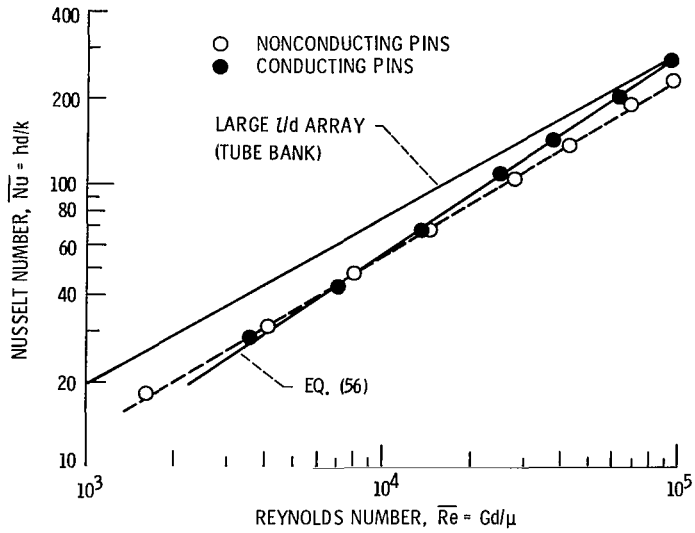

Figure 38. – Nusselt number as function of Reynolds number for $x_p/d = 2.5$. (From ref. 125.)

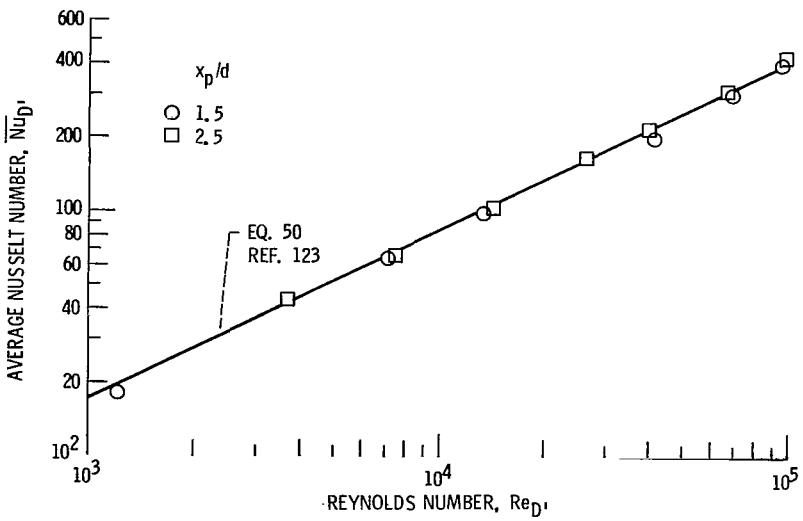

Figure 39. – Replot of data from figures 37 and 38, using characteristic dimension D' defined under equation (51). (From ref. 125.)

Concluding Remarks

Although published heat-transfer and, to a lesser extent, pressure-drop correlations are available for most of the general types of coolant passages used in turbine-blade design, areas still remain where more data are needed. Most of the correlations have been generated from data obtained at idealized inlet conditions, at low temperature and pressure, with uniform wall temperature, with uniform heating, and with fully developed flow. Examination of available literature showed that accuracies of the correlations are somewhere between ±10 percent and ±35 percent.

The following summarizes the results of this review on the status and needs for technology on heat transfer and pressure drop through internal passages in cooled turbine blades.

Convection Through Circular and Noncircular Passages

Correlations for fully developed, turbulent flows with idealized conditions, such as bellmouthed inlets or large plenums, are available (accuracy ±10 percent) to predict average heat transfer and pressure drop through passages. However, in actual turbine vane or blade designs, tortuous inlet paths and curved passage returns are the rule rather than the exception. Also, the passage lengths are such that the major portion of the flow is in the developing region. Although methods are available to account for the effects of developing flow at the inlet, these are mostly for idealized conditions and straight inlets. Little or no published experimental data are available for tightly curved returns, such as those used in the multipass passages. The little information that is available showed that the effect of passage curvature is to increase both the pressure-drop and average heat-transfer coefficients. For a tightly curved return typical of that used in turbine-blade designs, unpublished data show that the heat-transfer coefficients downstream of the return increased by a factor of about 2. Published information for heat transfer on the curved walls usually pertains to low heat flux conditions; whereas, the suction and pressure surface of the turbine blade walls are subject to high heat fluxes from the hot gas stream. Research is therefore needed to develop methods and correlations to predict local heat transfer and pressure drop in the passage returns. Research is also needed to include the effects of nonuniform peripheral heating of both circular and noncircular passages, especially for noncircular passages with sharp included angles between the walls, where the presence of stagnant flow zones may lower the local heat-transfer coefficients substantially below the periphery averaged values and create hot spots.

Rotation

Although some excellent analytical and experimental work has been done at low centrifugal and buoyancy conditions, the effect of centrifugal and buoyancy forces at high heat flux and high rotational speeds still requires verification. These buoyancy forces can negate or augment the heat-transfer process in the cooled passages. While empirical correlations have been obtained for the average heat-transfer coefficient in a tube for both radial coolant outflow and radial coolant inflow, further research is needed to expand the analytical predictive capabilities and to extend the experiments to higher Rayleigh and Reynolds numbers expected in advanced gas turbine engines.

Research is also needed on the effects of rotation on coolant passages with turbulators, especially in the undeveloped flow region and where the coolant passages are not radial to the axis of rotation (such as occurs at the leading and trailing edges of the airfoil). Because local metal temperatures are important to turbine-blade life, research is needed to obtain prediction methods and correlations for local heat-transfer coefficients along and around the rotating coolant passages, as well as for coolant pressure drops. High quality experiments are needed to help develop the prediction methods and correlations.

Impingement

Leading edge. – Much research has been done on impingement heat transfer in the leading-edge area. In one widely used reference, the experimentally obtained one-dimensional, spanwise averaged heat-transfer coefficients around the leading-edge area were stated to be within 8.7 percent of the given correlation equation, within the range of the experimental variables. Yet, the spread in the heat-transfer data obtained by this and other investigators at a given Reynolds number can differ by a factor of 3. Additional work is needed to obtain a more general correlation that would reduce the apparent differences among the various investigators. Only very limited information is available on the effect of leading-edge cavity shape on heat transfer, of multiple rows of impingement holes at the leading edge, and of bleeding the spent cooling air through film cooling holes. Further research is needed in these areas to develop prediction methods for local heat-transfer coefficients and metal temperatures in the leading-edge area.

Midchord. – Intensive research on impingement heat transfer on a flat plate tunnel using both in-line and staggered impingement hole configurations has resulted in a correlation of experimental, spanwise averaged Nusselt numbers that agreed to within 12 percent. As part

of planned research, the pressure-drop data will also be correlated for the same geometric and flow conditions as those used in the heat-transfer tests. The heat-transfer results already published and the planned pressure-drop correlations should satisfy the current requirements for one-dimensional prediction method for the turbine-blade midchord region. Other areas that needed attention are the effects of venting the spent air through film-cooling holes on heat transfer, the effects of curvature of the airfoil, and whether the effects of high turbine wall-to-coolant temperature ratios are significant to heat transfer. Research is also needed to determine the two dimensional heat transfer over the impinged surface because of the concern over possible large thermal gradients in the turbine blades during engine operation.

Enhanced Heat Transfer

Turbulators. – A number of publications have dealt with the effect of repeated rib type roughness on heat transfer and pressure drop. The correlations for both heat transfer and pressure drop agreed well (estimated to be within 10 percent) with experimental data for the range of experimental variables investigated. In view of the increasing popularity of the repeated rib design, particularly in multipass passage blades, work is needed to determine the combined effects on local heat transfer and pressure drop of the turbulators when coupled with entrance and turning effects. Other areas where research is needed include the effect of noncircular passages, and rotation, as mentioned earlier.

Pins. – Most available correlations were obtained by using data from tube bundles in cross flow for heat exchangers. The length-to-diameter l/D ratios of the tubes (or pins) are generally greater than than those used in turbine-blade designs for the thin trailing-edge region. A recent publication on four rows of short pins with length-to-diameter ratios of 2 and 0.5, typical of those used in turbine-blade cooling applications indicated the average heat-transfer coefficients can be lower by as much as a factor of 2 when compared with other data obtained from larger pin l/D ratios.

The data from this limited experiment on small l/D pins were correlated by an equation that used only the Reynolds number. Apparently, the effect of l/D in the range of 0.5 and 2 was not measurable. The current status with small l/D ratio pins is such that considerable research is needed to obtain a clearer understanding of the influence of geometric variables on both heat transfer and pressure drop. Some research is under way in these areas.

Not mentioned above, but sorely needed, is development of instrumentation that will provide accurate local measurements of flow conditions and heat transfer in both nonrotating and rotating environments. More accurate benchmark data are needed at low temperature and pressure conditions that simulate gas-turbine conditions for fundamental studies that contribute to the development of more accurate heat-transfer and pressure-drop prediction models and correlations. More accurate measurements are needed at high temperature and pressure gas conditions to evaluate and/or verify the accuracies of these prediction models and correlations at near engine conditions.

References

General

1. Stepka, F. S.: Analysis of Uncertainties in Turbine Metal Tem perature Predictions. NASA TP-1593, Apr. 1980.
2. Stepka, F. S.: NASA Thermal Barrier Coatings – Summary and Update. NASA TM X-79053, 1978.

Convection Circular Passages

3. Siegel, R.; and Sparrow, E. M.: Comparison of Turbulent Heat Transfer Results for Uniform Wall Heat Flux and Uniform Wall Temperature. J. Heat Transfer, vol. 82, no. 2, May 1980, pp. 152-153.
4. Dittus, F. W.; and Boelter, L. M. K.: Heat Transfer in Automobile Radiators of the Tubular Type. Univ. Calif., Berkeley, Publ. Eng., vol. 2, no. 13, 1930, pp. 443-461.
5. Petukhov, B. S.; and Popov, V. N.: Theoretical Calculation of Heat Exchange and Frictional Resistance in Turbulent Flow in Tubes of an Incompressible Fluid with Variable Physical Properties. High Temp., Engl. Transl., vol. 1, no. 1, July/Aug. 1963, pp. 69-83.
6. Webb, R. L.: A Critical Evaluation of Analytical Solutions and Reynolds Analogy Equations for Turbulent Heat and Mass Transfer in Smooth Tubes. Waeme Stoffubertrag., vol. 4, no. 4, 1971, pp. 197-204.
7. Humble, L. V.; Lowdermilk, W. H.; and Desmond, L. G.: Measurements of Average Heat Transfer and Friction Coefficients for Subsonic Flow of Air in Smooth Tubes at High Surface and Fluid Temperatures. NACA Report 1020, 1951.
8. McEligot, D. M.; Magee, P. M.; and Leppert, G.: Effect of Large Temperature Gradients on Convective Heat Transfer: The Downstream Region. J. Heat Transfer, vol. 87, no. 1, Feb. 1965, pp. 67-73.
9. Taylor, M. F.: Experimental Local Heat Transfer And Average Friction Data for Hydrogen and Helium Flowing in a Tube at Surface Temperatures up to 5600° R. NASA TN D-2280, 1964.
10. Taylor, M. F.: Experimental Local Heat Transfer Data for Precooled Hydrogen and Helium at Surface Temperatures up to 5300° R, NASA TN D-2595, 1965.
11. Taylor, M. F.: A Method of Correlating Local and Average Friction Coefficients for both Laminar and Turbulent Flow of Gases through a Smooth Tube with Surface to Fluid Bulk Temperature Ratios from 0.35 to 7.35. Int. J. Heat and Mass Transfer, vol. 10, pp. 1123-1128, Oct. 1967.

12. Wolf, H.: The Experimental and Analytical Determination of the Heat Transfer Characteristics of Air and Carbon Dioxide in the Thermal Entrance Region of a Smooth Tube with Large Temperature Differences Between the Gas and the Tube Wall. Ph.D. Thesis, Purdue University, 1958.
13. McEligot, D. M.: Effect of Large Temperature Gradients on Turbulent Flow of Gases in the Downstream Region of Tubes. TR 247-5, Stanford University, 1963.
14. Magee, P. M.: The Effect of Large Temperature Gradients on the Turbulent Flow of Gases in the Thermal Entrance Region of Tubes. TR 247-4, Stanford University, 1964.
15. Perkins, H. C.; and Worsoe-Schmidt, P.: Turbulent Heat and Momentum Transfer for Gases in a Circular Tube at Wall-to-Bulk Temperature Ratios to Seven. Int. J. Heat Mass Transfer, vol. 8, 1965, pp. 1011-1034.
16. McCarthy, J. R.; and Wolf, H.: The Heat Transfer Characteristics of Gaseous Hydrogen and Helium. Research Report RR-60-12, Rocketdyne, Dec. 1960.
17. Dalle Donne, M.; and Bowditch, F. H.: High Temperature Heat Transfer. Nucl. Eng., vol. 8, no. 1, Jan. 1963, pp. 20-29.
18. Weiland, W. F.: Measurement of Local Heat Transfer Coefficients for Flow of Hydrogen and Helium in a Smooth Tube at High Surface-to-Fluid Bulk Temperature Ratios. Chem. Eng. Prog. Symp. Ser., vol. 61, no. 60, 1965, pp. 97-105.
19. Petukhov, B. S.: Heat Transfer and Friction in Turbulent Pipe Flow with Variable Physical Properties. Advances in Heat Transfer, vol. 6, J. P. Hartnett and T. E. Irvine, Jr., eds., Academic Press, Inc., 1970, pp. 503-564.
20. Sleicher, C. A.; and Rouse, M. W.: A Convenient Correlation for Heat Transfer to Constant and Variable Property Fluids in Turbulent Pipe Flow. Int. J. Heat Mass Transfer, vol. 18, May 1975, pp. 677-683.
21. Simoneau, R. J.; and Hendricks, R. C.: A Simple Equation for Correlating Turbulent Heat Transfer to a Gas. NASA TM X-52011, 1964.
22. Black, A. W.; and Sparrow, E. M.: Experiments on Turbulent Heat Transfer in a Tube with Circumferentially Varying Thermal Boundary Conditions. J. Heat Transfer, vol. 89, no. 3, Aug. 1967, pp. 258-268.
23. Sparrow, E. M.; and Lin, S. H.: Turbulent Heat Transfer in a Tube with Circumferentially Varying Temperature and Heat Flux. Int. J. Heat Mass Transfer, vol. 6, Sept. 1963, pp. 866-867.
24. Davenport, M. E.; and Leppert, G.: The Effect of Transverse Temperature Gradients on the Heat Transfer and Friction for Laminar Flow of Gases. J. Heat Transfer, vol. 87, no. 2, May 1965, pp. 191-196.
25. Hendricks, R. C.: Bulk Expansion Factors and Density Fluctuations in Heat and Mass Transfer. Presented at the XV International Congress of Refrigeration, Venezia, Sept. 23-29, 1979.
26. Deissler, R. G.; and Eian, C. S.: Analytical and Experimental Investigation of Fully Developed Turbulent Flow of Air in a Smooth Tube with Heat Transfer with Variable Fluid Properties. NACA TN-2629, 1952.
27. Knowles, G. R.; and Sparrow, E. M.: Local and Average Heat Transfer Characteristics For Turbulent Air Flow in an Asymmetrically Heated Tube. J. Heat Transfer, vol. 101, no. 4, Nov. 1979, pp. 635-641.
28. Kays, W. M.; and Perkins, H. C.: Forced Convection Internal Flow in Ducts. Handbook of Heat Transfer, W. M. Rohsenow and J. P. Hartnett, eds., McGraw-Hill Book Co., 1973, pp. 7-1 to 7-193.
29. Eckert, E. R. G.; and Drake, R. M.: Analysis of Heat and Mass Transfer. McGraw-Hill Book Co., 1972.
30. Deissler, R. G.; and Taylor, M. F.: Analysis of Turbulent Flow and Heat Transfer in Non-Circular Passages. NACA TN-4384, 1958.
31. Emery, A. F.; Neighbors, P. K.; and Gessner, F. B.: The Numerical Prediction of Developing Turbulent Flow and Heat Transfer in a Square Duct. J. Heat Transfer, vol. 102, no. 1, Feb. 1980, pp. 51-57.
32. Eckert, E. R. G.; and Irvine Jr., T. F.: Pressure Drop and Heat Transfer in a Duct with Triangular Cross-Section. J. Heat Transfer, vol. 82, no. 2, May 1960, pp. 125-138.
33. Carlson, L. W.; and Irvine Jr., T. F.: Fully Developed Pressure Drop in Triangular Shaped Ducts. J. Heat Transfer, vol. 83, no. 4, Nov. 1961, pp. 441-444.
34. Ainsworth, R. W.; and Jones, T. V.: Measurements of Heat Transfer in Circular, Rectangular, and Triangular Ducts, Representing Typical Turbine Blade Internal Cooling Passages Using Transient Techniques. ASME paper 79-GT-40, Mar. 1979.
35. Altemani, C. A.: Turbulent Heat Transfer and Fluid Flow Characteristics for Air Flow in an Unsymmetrically Heated Triangular Duct. Ph. D. Thesis, University of Minnesota, 1980.
36. Malak, J.; Hejna, J.; and Schmid, J.: Pressure Losses and Heat Transfer in Non-Circular Channels with Hydraulically Smooth Walls. Int. J. Heat Mass Transfer, vol. 18, Jan. 1975, pp. 139-149.
37. Hartnett, J. P.; Koh, J. C. Y.; and McComas, S. T.: A Comparison of Predicted and Measured Friction Factors for Turbulent Flow Through Rectangular Ducts. J. Heat Transfer, vol. 84, no. 1, Feb. 1962, pp 82-88.
38. Lowdermilk, W. H.; Weiland, W. F.; and Livingood, J. N. B.: Measurement of Heat Transfer and Friction Coefficients for Flow of Air in Non-Circular Ducts at High Surface Temperatures. NACA RM E53J07, 1954.
39. Campbell, D. A.; and Perkins, H. C.: Variable Property Turbulent Heat and Momentum Transfer for Air in a Vertical Rounded Corner Triangular Duct. Int. J. Heat Mass Transfer, vol. 11, June 1968, pp 1003-1012.
40. Battista, E.; and Perkins, H. C.: Turbulent Heat and Momentum Transfer in a Square Duct with Moderate Property Variations. Int. J. Heat and Mass Transfer, vol. 13, June 1970, pp. 1063-1065.
41. Ramachandra, V.; and Spalding, D. B.: Fluid Flow and Heat Transfer of Rectangular-Sectioned Ducts. Report HTS/76/21, Department of Mechanical Engineering, Imperial College of Science and Technology, London, Nov. 1976.
42. Alexopoulos, C. C.: Temperature and Velocity Distributions and Heat Transfer for Turbulent Air Flow in a Vertical Square Duct. M. A. Sc. Thesis, Department of Mechanical Engineering, University of Toronto, 1964.
43. Allen, J.; and Grundberg, N. D.: Resistance to Flow of Water Along Smooth Rectangular Passages, and Effect of Slight Convergence or Divergence of the Boundaries. Philos. Mag. J. Sci., vol. 23, no. 154, Mar. 1937, pp. 490-503.
44. Cornish, R. J.: Flow in a Pipe of Rectangular Cross Section. Proc. R. Soc. of London, Ser. A, vol. 120, 1928, pp. 691-700.
45. Huebscher, P. S.: Friction Equivalents for Round, Square, and Rectangular Ducts. Heat./Piping/Air Cond., vol. 19, Dec. 1947, pp. 127-135.
46. Whan, G. A.; and Rothfus, R. R.: Characteristics of Transition Flow Between Parallel Plates. AIChE J., vol. 5, no. 2, June 1959, pp. 204-208.
47. Eckert, E. R. G.; and Irvine Jr., T. F.: Incompressible Friction Factor, Transition and Hydrodynamic Entrance-Length Studies of Ducts with Triangular and Rectangular Cross Sections. Proc.

Fifth Midwestern Conference on Fluid Mechanics, University of Michigan, 1957, pp. 122–145.
48. Schiller, L.: Die Entwicklung der laminaren Geschwindigkeitsvertelung und ihre Bedeuntung fur Zahigkeitsmessungen (Investigation on Laminar and Turbulent Flow). Z. Angew. Math. Mech., vol. 2, 1922, p.96.
49. Nikuradse, J.: Untersuchungen uber turbulente Stromungen in nicht Kreisformigen Kohren (Investigation of Turbulent Flow in Tubes of Non-Circular Cross Section). Ing. Arch., vol. 1, 1930, pp. 306–332.
50. Lea, F. C.: Flow of Water Through a Circular Tube With a Central Core and Through Rectangular Tubes. Phil. Mag. J. Sci., vol. 11, no. 74, June 1931, pp. 1235–1247.
51. Washington, L.; and Marks, W. M.: Heat Transfer and Pressure Drop in Rectangular Air Passages. Ind. Eng. Chem., vol. 29, no. 3, Mar. 1937, pp. 337–345.
52. Davies, S. C.; and White, C. M.: An Experimental Study of the Flow of Water in Pipes of Rectangular Section. Proc. R. Soc. London, Ser. A, vol. 119, 1928, pp. 92–106.
53. Jones, O. C. Jr.: An Improvement in Calculation of Turbulent Friction in Rectangular Ducts. J. of Fluids Eng., vol. 98, no. 2, June 1976, pp. 173–181.

Convection – Entrance Effects

54. Reynolds, H. C.; Swearingen, T. B.; and McEligot, D. M.: Thermal Entry for Low Reynolds Number Turbulent Flow. J. Basic Eng., vol. 91, no. 1, Mar. 1969, pp. 87–94.
55. Sparrow, E. M.; Hallman, T. M.; and Siegel, R.: Turbulent Heat Transfer in the Thermal Entrance Region of a Pipe with Uniform Heat Flux. Appl. Sci. Res., Sect. A, vol. 7, 1958, pp. 37–52.
56. Reynolds, H. C.; Davenport, M. E.; and McEligot, D. M.: Velocity Profiles and Eddy Diffusivities for Fully Developed, Turbulent, Low Reynolds Number Pipe Flow. ASME paper 68-WA/FE-34, Dec. 1968.
57. Campbell, W. D.; and Slattery, J. C.: Flow in Entrance of a Tube. J. Basic Eng., vol. 85, no. 1, Mar. 1963, pp. 41–46.
58. Sukomel, A. S.; et al.: An Investigation of Heat Transfer at the Initial Sector of a Flat Channel. Teploenergetika, vol. 22, no. 3, Mar. 1975, pp. 81–83.
59. Barbin, A. R.; and Jones, J. B.: Turbulent Flow in the Inlet Region of a Smooth Pipe. J. Basic Eng., vol 85, no. 1, Mar. 1963, pp. 29–34.
60. Benedict, J. S.; et al.: Generalized Flow Across an Abrupt Enlargement. J. Eng. Power, vol. 98, no. 3, July 1976, pp. 327–334.
61. Hughmark, G. A.: Heat, Mass, and Momentum Transport with Turbulent Flow in Smooth and Rough Pipes. AIChE J., vol. 21, no. 5, 1975, pp. 1033–1035.
62. Boelter, L. M. K.; Young, G.; and Iversen, H. W.: An Investigation of Aircraft Heaters. XXVII – Distribution of Heat Transfer Rate in the Entrance Section of a Circular Tube. NACA TN-1451, 1948.
63. Deissler, R. G.: Analysis of Turbulent Heat Transfer and Flow in the Entrance Regions of Smooth Passages. NACA TN-3016, 1953.

Convection – Rotational Effects

64. Skiadaressis, D.; and Spalding, D. B.: Heat Transfer in Ducts Rotating Around A Perpendicular Axis. Sixth International Heat Transfer Conference, vol. 2, National Research Council of Canada, 1978, pp. 91–95.
65. Skiadaressis, D.; and Spalding, D. B.: Heat Transfer in a Pipe Rotating Around A Perpendicular Axis. ASME Paper 77-WA/HT-39, 1977.
66. Mori, Y.; Fukada, T.; and Nakayama, W.: Convective Heat Transfer in a Rotating radial Circular Pipe (2nd Report). Int. J. Heat Mass Transfer, vol. 14, no. 11, Nov. 1971, pp. 1807–1824.
67. Morris, W. D.: Flow and Heat Transfer in Rotating Coolant Channels High Temperature Problems in Gas Turbines, AGARD-CP-229, Feb. 1978.
68. Ito, H.; and Nanbu, K.: Flow in Rotating Straight Pipes of Circular Cross Section. J. Basic Eng., vol. 93, no. 3, Sept. 1971, pp. 383–394.
69. Moore, J.: Report No. 89, Gas Turbine Laboratory, M.I.T., 1967.
70. Lokai, V. I.; and Limanski, A. S.: Influence of Rotation on Heat Transfer in Radial Cooling Channels of Turbine Blades. Aviats. Tekh., vol. 18, no. 3, 1975, pp. 69–72.
71. Zysina-Molozhen, L. M.; Dergach, A. A.; and Kogan, G. A.: Experimental Investigation of Heat Transfer in a Radially Rotating Pipe. High Temp., vol. 14, no. 4, July/Aug. 1976, pp. 988–991.
72. Trefethen, L.: Flow in Rotating Radial Ducts. General Electric Co. Report 55GL 350-A, 1957.
73. Majumdar, A. K.; Pratap, V. S.; and Spalding, D. B.: Numerical Computation of Flow in Rotating Ducts. J. Fluids Eng., vol. 99, no. 1, Mar. 1977, pp. 148–153.
74. Majumdar, A. K.; and Spalding, D. B.: A Numerical Investigation of Three-Dimensional Flows in a Rotating Duct by a Partially Parabolic Procedure. ASME Paper 77-WA/FE-7, 1977.
75. Howard, J. H. G.; Patankar, S. V.; and Bordynuik, R. M.: Flow Prediction in Rotating Ducts Using Coriolis-Modified Turbulence Models. J. Fluids Eng., vol. 102, no. 4, Dec. 1980, pp. 456–461.
76. Morris, W. D,; and Ayhan, T.: Observations on the Influence of Rotation on Heat Transfer in the Coolant Channels of Gas Turbine Rotor Blades. Proc., Inst. Mech. Eng., London, vol. 193, Sept. 1979, pp. 303–312.
77. Morris, W. D.: Heat Transfer and Fluid Flow in Rotating Coolant Channels. John Wiley & Sons, Ltd., 1981.
78. Chupp, R. E.; et al.: Evaluation of Internal Heat Transfer Coefficient for Impingement-Cooled Turbine Airfoils. J. Aircr., vol. 6, no. 3, May-June 1969, pp. 203–208.
79. Metzger, D.; E.; Baltzer, R. T., and Jenkins, C. W.: Impingement Cooling Performance in Gas Turbine Airfoils Including Effects of Leading Edge Sharpness. J. Eng. Power, vol. 94, no. 3, July 1972, pp. 219–225.
80. Metzger, D. E.; Yamashita, T.; and Jenkins, C. W.: Impingement Cooling of Concave Surfaces with Lines of Circular Air Jets. J. Eng. Power, vol. 91, no. 3, July 1969, pp. 149–158.
81. Jenkins, C. W.; and Metzger, D. E.: Local Heat Transfer Characteristics of Concave Cylindrical Surfaces Cooled by Impinging Slot Jets and Lines of Circular Jets with Spacing Ratios 1.25, to 6.67. Tech Rep. ME-694, Arizona State Univ., May 1969.
82. Damerow, W. P.; Murtaugh, J. P.; and Burggraf, F.: Experimental and Analytical Investigation of the Coolant Flow Characteristics in Cooled Turbine Airfoils. (GE-R72-AEG-165, General Electric Co.; NASA Contract NAS3-13499). NASA CR-120883, June 1972.
83. Livingood, J. N. B.; and Gauntner, J. W.: Average Heat Transfer Characteristics of a Row of Circular Air Jets Impinging on a Concave Surface. NASA TM X-2657, Oct. 1972.

84. Jusionis, V. J.: Heat Transfer from Impinging Gas Jets on an Enclosed Concave Surface. J. Aircr., vol. 7, no. 1, Jan.-Feb. 1970, pp. 87–88.
85. Burggraf, F.: Average Heat Transfer Coefficients with a Row of Air Jets Discharging into a Half Cylinder. MS Thesis, U. Cincinnati, 1967.
86. Livingood, J. N. B.; and Gauntner, J. W.: Local Heat Transfer Characteristics of a Row of Circular Air Jets Impinging on a Concave Semi-Cylindrical Surface. NASA TN D-7127, Jan. 1973.
87. Arsen'yev, L. V.; and Mitryayev, I. B.: Effect of Duct Geometry on the Heat Transfer at the Inlet Edge of a Blade Cooled by an Array of Individual Jets. Heat Transfer, Sov. Res., vol. 8, no. 3, May-June, 1976, pp. 122–127.
88. Dyban, Ye P.; and Mazur, A. I.: Heat Transfer From a Flat Air Jet Flowing into a Concave Surface. Heat Transfer, Sov. Res., vol. 2, no. 3, May 1970, pp. 15–20.
89. Ravuri, R; and Tabakoff, W.: Heat Transfer Characteristics of a Row of Air Jets Impinging on the Inside of a Semi-Circular Cylinder. Report THEMIS-AE-71-18, U. Cincinnati, Jan. 1971, (AD-718794).
90. Burggraf, F.: Local Heat Transfer Coefficient Distribution with Air Impingement into a Cavity. ASME paper 72-GT-59, Mar. 1972.

Impingement – Midchord

91. Kercher, D. M.; and Tabakoff, W.: Heat Transfer by a Square Array of Round Air Jets Impinging Perpendicular to a Flat Surface Including the Effect of Spent Air. J. Eng. Power, vol. 92, no. 1, Jan. 1970, pp. 73–82.
92. Gardon, R.; and Cobonque, J.: Heat Transfer Between a Flat Plate and Jets of Air Impinging on It. International Developments in Heat Transfer, Proceedings of 2nd. Internal Heat Transfer Conference, ASME, 1962, pp. 454–460.
93. Gardon, R.; and Akfirat, J. C.: The Role of Turbulence in Determining the Heat Transfer Characteristics of Impinging Jets. Int. J. Heat Mass Transfer, vol. 8, Sept. 1965, pp. 1261–1272.
94. Metzger, D. E.; and Korstad, R. J.: Effects of Cross Flow in Impingement Heat Transfer. J. Eng. Power, vol. 94, no. 1, Jan. 1972, pp. 35–41.
95. Huang, G. C.: Investigations of Heat Transfer Coefficients for Air Flow Through Round Jets Impinging Normal to a Heat-Transfer Surface. J. Heat Transfer , vol. 85, no. 3, Aug. 1963, pp. 237–243.
96. Friedman, S. J.; and Mueller, A. C.: Heat Transfer to Flat Surfaces. Proceedings, General Discussion on Heat Transfer. The Institute of Mechanical Engineers, London, 1951, pp. 138–142.
97. Chance, J. L.: Experimental Investigation of Air Impingement Heat Transfer Under an Array of Round Jets. Tappi, vol. 57, no. 6, June 1974, pp. 108–112.
98. Bouchez, J. P.; and Goldstein, R. J.: Impingement Cooling from a Circular Jet in a Crossflow. Int. J. Heat Mass Transfer, vol. 18, June 1975, pp. 719–730.
99. Gauntner, J. W.; et al.: Cross Flow Effects on Impingement Cooling of a Turbine Vane. NASA TM X-3029, Mar. 1974.
100. Sparrow, E. M.; Goldstein, R. J.; and Rouf, M. A.: Effect of Nozzle-Surface Separation Distance on Impingement Heat Transfer for a Jet in a Crossflow. J. Heat Transfer, vol. 97, no. 4, Nov. 1975, pp. 528–533.
101. Martin, H.: Heat and Mass Transfer Between Impinging Gas Jets and Solid Surfaces. Advances in Heat Transfer, vol. 13, J. P. Hartnett and T. F. Irvine, eds. Academic Press, 1977, pp. 1–60.
102. Hollworth, B. R.; and Dagan, L.: Arrays of Impinging Jets with Spent Fluid Removed Through Vent Holes on the Target Surface. Part 1. Average Heat Transfer. ASME paper 80-GT-42, Mar. 1980.
103. Hollworth, B. R.; Lehmann, G.; and Rosiczkowski, J.: Arrays of Impinging Jets With Spent Fluid Removal Through Vent Holes on the Target Surface. Part 2: Local Heat Transfer. ASME paper 81-HT-76, Aug. 1981.
104. Holworth, B. R.; and Berry, R. D.: Heat Transfer from Arrays of Impinging Jets with Large Jet-to-Jet Spacing. ASME paper 78-GT-117, Apr. 1978.
105. Colladay, R. S.: Turbine Cooling. Turbine Design and Applications. Arthur J. Glassman, ed., NASA SP-290, vol. 3, 1975, pp. 59–101.
106. Florschuetz, L. W.; et al.: Multiple Jet Impingement Heat Transfer Characteristics – Experimental Investigation of Inline and Staggered Arrays with Crossflow. NASA CR-3217, Jan. 1980.
107. Florschuetz, L. W.; Metzger, D. E.; and Truman, C. R.: Jet Array Impingement with Crossflow – Correlation of Streamwise Resolved Flow and Heat Transfer Distribution. NASA CR-3373, Jan. 1981.
108. Florschuetz, L. W.; and Isoda, Y.: Flow Distributions and Discharge Coefficient Effects for Jet Array Impingement with Initial Cross Flow. ASME paper 82-GT-156, Apr. 1982.
109. Dyban, E. P.; Mazur, A. I.; and Golovanov, V. P.: Heat Transfer and Hydrodynamics of an Array of Round Impinging Jets with One-Sided Exhaust of the Spent Air. Int. J. of Heat Mass Transfer, vol. 23, May 1980, pp. 667–676.
110. Saad, N. R.; et al.: Local Heat Transfer Characteristics for Staggered Arrays of Circular Impinging Jets with Cross Flow of Spent Air. ASME paper 80-HT-23, July 1980.

Enhanced Heat Transfer – artificially roughened surfaces (Turbulators)

111. Dipprey, D. F.; and Sabersky, R. H.: Heat and Momentum Transfer in Smooth and Rough Tubes at Various Prandtl Numbers. Int. J. Heat Mass Transfer, vol. 6, May 1963, pp. 329–353.
112. Webb, R. L.: Turbulent Heat Transfer in Tubes Having Two-Dimensional Roughness, Including the Effect of Prandtl Number. Ph. D. Thesis, Univ. of Minnesota, 1969.
113. Han, J. C.; Glickman, L. R.; and Rohsenow, W. M.: An Investigation of Heat Transfer and Friction for Rib-Roughened Surfaces. Int. J. Heat and Mass Transfer, vol. 21, Aug. 1978, pp. 1143–1156.
114. Kader, B. A.; and Yaglom, A. M.: Turbulent Heat and Mass Transfer from a Wall with Parallel Roughness Ridges. Int. J. Heat Mass Transfer, vol. 20, Apr. 1977, pp. 345–357.
115. Bergles, A. E.: Survey and Evaluation of Techniques to Augment Convective Heat and Mass Transfer. Progress in Heat and Mass Transfer, vol. 1, U. Griguli: and E. Hahne, eds., Pergamon Press, Ltd., 1969, pp. 331–424.
116. Kalinin, E.; et al.: The Experimental Study of the Heat Transfer Intensification Under Conditions of Forced One-and Two-Phase Flow in Channels. Augmentation of Convective Heat and Mass Transfer, ASME, 1970, pp. 80–90.
117. Donni, M. D.; and Meyer, L.: Turbulent Convective Heat Transfer From Rough Surfaces with Two-Dimensional Rectangular Ribs. Int. J. Heat Mass Transfer, vol. 20, June 1977, pp. 583–620.

118. Gomelauri, V. I.: Methods and Results of an Experimental Investigations of the Process of Intensification of Convective Heat Transfer. Teploenergetika, vol. 21, no. 9, 1974, pp. 2-5.

Enhanced Heat Transfer – Pins

119. Theoclitus, G.: Heat Transfer and Flow Friction Characteristics of Nine Pin Fin Surfaces. J. Heat Transfer, vol. 88, no. 4, Nov. 1966, pp. 383-390.
120. Zukauskas, A.: Heat Transfer from Tubes in Cross Flow. Advances in Heat Transfer, vol. 8, J. P. Hartnett and T. F. Irvine, Jr., eds., Academic Press, Inc., 1972, pp 93-160.
121. Faulkner, F. E.: Analytical Investigation of Chord Size and Cooling Methods on Turbine Blade Cooling Requirements. (AIRESEARCH 71-7487-BK-1, AiResearch Mfg. Co.; NASA Contract NAS3-13205). NASA CR-120882-BK-1, Aug. 1971.
122. Jakob, M.: Heat Transfer and Flow Resistance in Cross Flow of Gases over Tube Banks. Trans ASME, vol. 60, 1938, pp. 384-386.
123. Van Fossen, G. J.: Heat Transfer Coefficients for Staggered Arrays of Short Pin Fins. NASA TM-81596, 1981.
124. Simoneau, R. J., and Van Fossen, G. J., Jr.: Effect of Location in an Array on Heat Transfer to a Cylinder in Crossflow. NASA TM X-82797, 1982.
125. Metzger, D. E.; and Haley, S. W.: Heat Transfer Experiments and Flow Visualization for Arrays of Short Pin Fins. ASME paper 82-GT-138, Apr. 1982.
126. Brown, A.; Mandjikas, B.; and Mudyiwa, J. M.: Blade Trailing Edge Heat Transfer. ASME paper 80-GT-45, Mar. 1980.
127. Kays, W. M.; and London, A. L.: Compact Heat Exchangers. National Press, Palo Alto, Calif., 1955.

1. Report No.	2. Government Accession No.	3. Recipient's Catalog No.
NASA TP-2232		

4. Title and Subtitle

Review and Status of Heat-Transfer Technology for Internal Passages of Air-Cooled Turbine Blades

5. Report Date: April 1984

6. Performing Organization Code: 505-32-2B

7. Author(s)

Frederick C. Yeh and Francis S. Stepka

8. Performing Organization Report No.: E-1373

10. Work Unit No.

9. Performing Organization Name and Address

National Aeronautics and Space Administration
Lewis Research Center
Cleveland, Ohio 44135

11. Contract or Grant No.

13. Type of Report and Period Covered: Technical Paper

12. Sponsoring Agency Name and Address

National Aeronautics and Space Administration
Washington, D.C. 20546

14. Sponsoring Agency Code

15. Supplementary Notes

16. Abstract

A review of turbine blade coolant-side heat-transfer technology is needed as inaccuracies in many of the correlations or extrapolations of correlations can result in large errors in the prediction of turbine-blade metal temperatures and life. Designers have often used correlating heat-transfer and flow equations because of a general acceptance of its usage and do not have the time in inquire about the inaccuracies of the correlations, the conditions, and the range of applicability. This report presents a review of selected literature on heat-transfer and pressure losses for airflow through passages for several cooling methods generally applicable to gas turbine blades. The review highlights some useful correlating equations, discusses the status of turbine-blade internal air-cooling technology for both nonrotating and rotating blades and points out the areas where further research is needed. The cooling methods considered include convection cooling in passages, impingement cooling at the leading edge and at the midchord, and convection cooling in passages, augmented by pin fins and the use of roughened internal walls.

17. Key Words (Suggested by Author(s))

Heat transfer
Turbomachinery
Turbine blades

18. Distribution Statement

Unclassified - unlimited
STAR Category 34

19. Security Classif. (of this report)	20. Security Classif. (of this page)	21. No. of pages	22. Price*
Unclassified	Unclassified	35	A02

*For sale by the National Technical Information Service, Springfield, Virginia 22161

NASA-Langley, 1984

3 1 1U,D, 840411 S00903DS
DEPT OF THE AIR FORCE
AF WEAPONS LABORATORY
ATTN: TECHNICAL LIBRARY (SUL)
KIRTLAND AFB NM 87116